Research status of replacement gases for SF_6 in power industry

Cite as: AIP Advances **10**, 050702 (2020); https://doi.org/10.1063/1.5134727
Submitted: 04 November 2019 • Accepted: 29 March 2020 • Published Online: 07 May 2020

Shuangshuang Tian, Xiaoxing Zhang, Yann Cressault, et al.

AIP Advances REVIEW scitation.org/journal/adv

Research status of replacement gases for SF_6 in power industry

Cite as: AIP Advances 10, 050702 (2020); doi: 10.1063/1.5134727
Submitted: 4 November 2019 • Accepted: 29 March 2020 •
Published Online: 7 May 2020

View Online Export Citation CrossMark

Shuangshuang Tian,[1] Xiaoxing Zhang,[1,a)] Yann Cressault,[2] Juntai Hu,[3] Bo Wang,[3] Song Xiao,[4] Yi Li,[4] and Narjisse Kabbaj[2]

AFFILIATIONS

[1] Hubei Key Laboratory for High-efficiency Utilization of Solar Energy and Operation Control of Energy Storage System, Hubei University of Technology, Wuhan 430068, China

[2] LAPLACE (Laboratoire Plasma et Conversion d'Energie), UPS, INPT, Université de Toulouse, 118 route de Narbonne, CO F-31062 Toulouse Cedex 9, France

[3] State Grid Pingdingshan Power Supply Company, Pingdingshan 467001, China

[4] School of Electrical Engineering, Wuhan University, Wuhan 430072, China

[a)] Author to whom correspondence should be addressed: xiaoxing.zhang@outlook.com

ABSTRACT

SF_6 is widely used in the industrial field due to its stable structure and excellent properties. It is mainly used in electrical insulation equipment. Due to the boiling point of SF_6, its use in extremely cold regions has been limited. It is harmful to the health of practitioners due to the toxicity of decomposition products. The gas has limited its wider use because of its strong greenhouse effect. As a result, researchers and electrical equipment manufacturing companies around the world are gradually searching for new environmentally friendly gases and have conducted research and exploration on theory and experiment. In this paper, the current status and existing problems of SF_6 are summarized. The research contents and research methods of SF_6 alternative gas direction are reviewed from the aspects of insulation performance, interrupter performance, and decomposition performance. The existing research results of the natural gas, SF_6 mixed gas, perfluorocarbons, and C_nF_mX gas are summarized, and the future development trend of alternative gas for SF_6 in the electrical industry is proposed.

I. INTRODUCTION

In 1900, an artificial inert gas called sulfur hexafluoride (SF_6) was synthesized by two French chemists, Moissan and Lebeau. SF_6 is composed of the most active elements in the halogen, fluorine (F) and sulfur (S) atoms.

The S atom is bonded by the sp3d2 hybrid orbit, and the molecular structure is an octahedron, in which the six F atoms are at the fixed position and the S atom is in the central position. S and F atoms are linked with covalent bonds, as shown in Fig. 1.[1] It has a stable chemical structure and strong insulation capacity, and the arc-extinguishing capacity of SF_6 is 100 times that of the air, and the insulation capacity is 2.5 times that of the air. It is a new ultra-high voltage dielectric insulation gas, which is superior to air and oil. Due to the excellent insulation properties and arc extinguishing performance, it is used in electrical equipment as gas-insulation media, such as circuit breakers, high voltage transformers, gas sealed combination capacitors, high voltage transmission lines, and transformers.

High purity SF_6 is an ideal electronic etchant, which is widely used in microelectronic technology. SF_6 is also used as a refrigerant in the refrigeration industry, and the refrigeration range can be between $-45\,^{\circ}$C and $0\,^{\circ}$C. SF_6 is used as an anti-adsorbent in the mining industry to replace oxygen in coal mine dust.

SF_6 is widely used in metal melting (such as magnesium alloy melting furnace protective gas), aerospace applications, medical applications (x-ray machine and laser), meteorological tracer analysis, chemical applications (senior car tires and new fire extinguishers), and so on. With the development of science and technology, the fields covered by SF_6 are constantly expanding more and more,

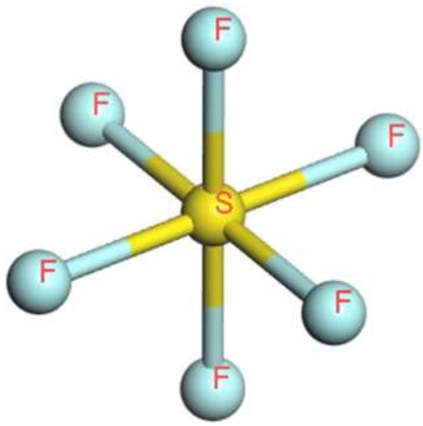

FIG. 1. Molecular structure of SF_6.

such as basic fields and science and technology fields. With the continuous development of the power grid and the gradual increase in the voltage level of the equipment, the usage of SF_6 is also gradually increasing. However, since SF_6 is a typical greenhouse gas and the demand for limiting its use is getting higher and higher, the research on alternative gases is going deeper and deeper. Of course, in addition to the greenhouse effect, the toxicity of SF_6 decomposition products and the boiling point are also factors that limit their use.

This paper reviewed the research status of SF_6 replacement gases in order to help researchers study the new substitute gases. This paper is organized as follows: Sec. II introduces the properties of SF_6, which is the important reason that it can be used widely in the power industry, and points out the disadvantages, which is the reason for looking for substitute gases. Section III focused on the main evaluation indices of alternative gases, such as the gas insulation, arc extinguishing, and decomposing properties. Section IV lists the research results of natural gases, SF_6 mixtures, perfluorocarbons, and other gases based on the evaluation indices in Sec. III. Section V shows the conclusion and outlook about the SF_6 replacement gases.

II. SF_6

A. The use and development of SF_6 in power industry

1. Insulation properties

SF_6 is not permanently broken down as solid insulation, and the insulating properties can be comparable to those of oil if the pressure is large enough, so it can be used in gas-insulated equipment. Under severe discharge and high temperatures, pure SF_6 is relatively stable and self-recovery performance is better, and no harmful solid impurities are precipitated by gas decomposition. Camilli and Chapman[2] compared various gases (SF_6, N_2, CF_2Cl_2, CF_3Cl, CF_4, $CHClF_2$, and CHF_2) by testing the lightning impulse voltage and the 60 Hz AC voltage. SF_6 was found to be the most ideal insulating gas in terms of the boiling point and insulation properties. It can maintain good insulation properties even at lower pressure. Camilli *et al.*[3] also explored the feasibility of using gas-insulated media in high-voltage transformers by analyzing the electrical properties and chemical properties. Compared with the transformer oil, the gas cooling capacity is relatively poor, so the application of SF_6 in the transformer may require an additional cooling system or increase in the volume of equipment. Menju *et al.*[4] studied the insulation properties of SF_6 in the gap between the ball electrode and the coaxial cylinder. By measuring the breakdown time T and the breakdown voltage V, it is considered that the VT curve (the abscissa represents T, and the ordinate represents V) of SF_6 is relatively flat, and the gas can well protect the device from over-voltage for a long time. This provides a theoretical basis for the application of SF_6 in gas-insulated transmission lines.

As the voltage level is gradually increased, the advantages of DC transmission equipment are obvious. The demand for gas-insulated equipment at DC voltage is driven. Menju and Takahashi[5] tested the DC breakdown characteristics of different electrodes and concluded that the combination of SF_6 gas and epoxy resin can be effectively used in the insulation system of a high voltage DC gas insulated substation. Rizk *et al.*[6] studied the movement characteristics of conductive particles between coaxial cylindrical electrodes and their effect on the DC breakdown voltage by experiments. They improved the model of particle motion in a coaxial field, considering that particles were subjected to charge accumulation and centrifugal forces.

For the microscopic parameters of gas discharge, Boyd and Crichton[7] measured the ionization coefficient and attachment coefficient of the SF_6 molecule, and these parameters provide important references for the study of the gas discharge process. In the range of 25 °C–125 °C, the temperature does not affect the electron attachment process of the gas molecules, but the increase in temperature would promote the diffusion process, thus changing the space charge distribution and eventually causing the breakdown voltage to rise.[8]

2. Arc extinguishing properties

The interruption ability of SF_6 was significantly higher than that of air.[9] In 1956, Cromer and Friedreich[10] found that the interruption ability of SF_6 was significantly higher than that of air, the arc extinguishing capacity of plain-break arcs at AC voltage was about 100 times of that of air, and the limiting current value of the arc extinguishing current had a rough linear relationship with the arc length and the gas pressure. The SF_6 circuit breaker could cut off the current of 5000 A at 115 kV. In 1957, Leeds *et al.*[11] measured the current change in SF_6 during quenching. By installing a cross-blast and arc-splitter, the interrupting current can be increased as demonstrated by Kane and Colclaser in 1963[12] in a 69-kV SF_6 common-tank breaker. They concluded that SF_6 as the interrupter medium results in a perfect switching and interruption effect. In 1964, Easley and Telford[13] designed a new type of circuit breaker, which was quenched by a new jet-type interruption structure. The interruption and impulse withstand tests of the new circuit breaker reached the standards of the American Standards Association (ASA).[14]

In 1965, the first SF_6 500 kV circuit breakers were started to be used in the USA.[15] 1550-kV basic insulation level (BIL) circuit breakers with SF_6 as the insulating gas also appeared one after another.[16] ASA (American Standards Association) reported the use of 115 kV–345 kV circuit breakers with SF_6 as the arc-extinguishing medium in terms of the mechanical structure, working principle, and arc extinguishing performance, and extended it to the corresponding extra high voltage (EHV) transmission lines.[17–21]

Due to its superior performance, SF_6 was considered as an insulating medium and arc-extinguishing medium in electrical equipment.[22] SF_6 is today widely used in the power industry in gas insulated circuit breakers (GCBs), gas insulated switchgears (C-GISs), gas insulated circuits (GILs), and gas insulated transformers (GITs),[23–30] and the current production of SF_6 is mainly used in the power industry, accounting for about 80% of the total production.[31]

Since then, SF_6 gas-insulated equipment has been developed and perfected for decades. SF_6 occupies an important position in the gas-insulated equipment, and the theoretical and experimental research on SF_6 has never been interrupted. For example, SF_6 is used as the insulation medium and arc extinguishing medium in the 1000 kV GIS, and the rated short-time withstand current reaches 50 kA. With the continuous development of the power grid and the gradual increase in the voltage level of the equipment, the usage of SF_6 is constantly increasing despite its disadvantages.

B. The disadvantages

In the recent decades, it has been found that there are mainly three problems about the use of SF_6 in electrical equipment. The first one is the boiling point, which cannot be used in electrical equipment in extremely cold areas. The second one is toxicity since SF_6 may be decomposed in the equipment to produce some toxic gases such as SO_2, SO_2F_2, SOF_2, and S_2F_{10}, which can react with metals to produce various metal sulfides. Finally, SF_6 is a typical greenhouse gas. With the increase of usage, the impact on the environment cannot be neglected. The content of SF_6 in the atmosphere increased by 20% from 2011 to 2016, which is also the most important reason for the urgent need to find a new type of green gas instead of SF_6. According to forecasts, by 2030, SF_6 emissions from the power sector alone will reach 64×10^6 metric tons of carbon dioxide equivalent (MtCO2e).[31] So, limiting their use and emissions has become the current requirement for environmental protection and sustainable development.

1. The boiling point

The boiling point of SF_6 is $-65\,^{\circ}$C (0.1 MPa). This temperature meets the operating requirements of most equipment, but liquefaction still persists in extremely cold regions, which needs a lower boiling point. In the initial gas-insulated equipment design and development phase, a variety of insulating gases were considered within the scope. All kinds of insulating gases were tested, and theoretical analysis was performed by research workers and electrical equipment companies such as General Electric (GE). The initial purpose of exploration has always been simpler, considering the insulating properties and the boiling point as the main purpose.

In 1980, Devins[32] from General Electric (GE) Company conducted research on the key parameters such as dielectric strength and boiling point of thousands of gases and screened out relatively high-performance insulating media. Most of the gases in the insulation strength and boiling point cannot reach the SF_6 level at the same time, but the impact on the environment is ignored. The research on the SF_6 gas mixture started earlier and almost at the same time as the research on SF_6 gas. It has been a hot topic, and it has been a breakthrough for the SF_6 gas mixture until 2000. The study found that the appropriate reduction in the SF_6 mixing ratio can meet the needs of equipment operation and solved the media liquefaction in the equipment. The SF_6 mixed gas was begun to be used in the GIL.

2. The toxicity of decomposition products

Even if a new SF_6 gas insulated device can be non-toxic, it may contain toxic gases after a certain period of operation.[33] Despite the good chemical inertness, the decomposition of SF_6 still occurs under the arc with low-fluoride sulfides (SF_2 and SF_4) produced by breaking the S–F bond. Under the conditions of high voltage and high temperature during discharge, SF_6 decomposes to form various free radicals, which can react with water, oxygen, and solid insulating material epoxy resin $[(C_{11}H_{12}O_3)_n]$ in equipment to form SO_2, SO_2F_2, SOF_2, and so on. A very small amount of water molecules and oxygen molecules (ppm level) is inevitable in high purity SF_6. Vanroggen *et al.*[34] noted that the reaction of SF_6 with other gases can produce toxic low-fluoride sulfides, as well as oxide SOx, and even the highly toxic S_2F_{10}, HF, and others. Vijk explored the reaction of SF_6 with the metal in the circuit breaker by simulating the environment of the circuit breaker and measuring the consumption of different metal electrodes.[35] Due to the impurities contained in SF_6, as well as metal and solid insulation materials in electrical equipment, the decomposition products also include CS_2, WF_6, and SiF_4.

Some substances are toxic gases and cause health problems to workers in the power industry. Kraut and Lilis[36] reported that six electrical workers were exposed to SF_6 decomposition products during electrical service for more than 6 h (within 12 h) without protection. Most notably, the decomposition gas has a significant effect on the lung function. The threshold values (TLVs) of the main decomposition products SF_4, S_2F_{10}, SO_2, SOF_2, SO_2F_2, and HF are also given. Pilling and Jones[37] described a series of symptoms of dyspnea, hemoptysis, and cyanosis when two power workers inhaled SF_6 decomposition products for on-site maintenance and pointed out that the main decomposition products of SF_6 has a direct effect on the alveolar capillary membrane, which might lead to pulmonary edema, hypoxemia, arrhythmia, and mild tissue acidosis based on the clinical observation. Table I shows the possible damage to the human body caused by the main gas decomposition products of SF_6.

3. The greenhouse effect

With the global warming, the use and emission of greenhouse gases have drawn more and more attention from all over the world. Obama pointed out in "Science" that if the greenhouse gas emission is not limited, the global average temperature may increase by $4\,^{\circ}$C or more by 2100.[41] The Kyoto Protocol in 1997 classified the types of greenhouse gases. It was clear that SF_6 is one of six greenhouse gases. It was required that the use of SF_6 should be gradually reduced by 2020.[42] The GWP value of SF_6 is about 23 900 times that of CO_2 with a lifetime of 3200 years. The content of SF_6 gas in the atmosphere has increased by 8.7% per year.[43] So far, the SF_6 gas accounts for more than 15% of the total greenhouse gas emissions. In 2005, the emissions of SF_6 and other F-containing gases reached 0.95 pg, which would reach 3.7 pg in 2050 keeping with the current

TABLE I. Main clinical symptoms caused by decomposition products of SF_6.[38–40] Notation: the TLV is a time-weighted average concentration at which no adverse health effects are expected, for exposure during 8 h/day, for up to 40 h/week, in ppm_{vol}.

The decomposition gases	Health effects	Threshold limit value (TLV) (ppm)
SF_2	Not toxic	...
SF_4	Corrosive: Inhalation, skin, eye, and ingestion. It can cause lung damage, which affects the respiratory system; its toxicity its toxicity is similar to phosgene toxicity	0.1
S_2F_2	Toxic and pungent smell. Destructive to the respiratory system	0.5
SOF_4	Corrosive: Inhalation, skin, and eye	0.5
S_2F_{10}	Vascular-shock Lungs, thorax, or respiration–acute pulmonary edema Blood—changes in the cell count (unspecified)	0.01
SO_2	Strong irritation to the upper respiratory tract and lungs. It is mainly used in the upper respiratory tract. A large number of acute exposure can cause pulmonary edema and respiratory paralysis.	2
SOF_2	It can cause severe pulmonary edema and mucous membrane irritation.	1.6
SO_2F_2	Inhalation of this odorless gas can quickly result in death.	5
HF	Very hazardous in the case of skin contact (corrosive and irritant), eye contact (irritant and corrosive), and ingestion. Inhalation of the spray mist may produce severe irritation of the spray mist may produce severe irritation of the respiratory tract, characterized by coughing, choking, or shortness of breath.	3
CS_2	Extremely hazardous in the case of skin contact (irritant), ingestion, and inhalation.	10
CO	It combines with hemoglobin in the blood to cause hypoxia.	50
WF_6	Very toxic and intensely irritating	0.1
SiF_4	Inhalation, skin, eye, and mucous membrane contact. High concentration exposures may produce pulmonary irritation, and low concentration exposures may produce generalized effects of fluorine exposure	0.6 0.6

emission levels.[44] Since 1997, the USA, Japan, and the EU countries have formulated policies and measures to limit the use of SF_6. California proposed that the use of SF_6 in the electrical field should be reduced year by year from 2020 and the EU plans to reduce SF_6 emissions to 2/3 of 2014 by 2030. Spain and Australia have increased the tax of SF_6 emissions. It can be said that the main reason for the research on SF_6 alternative gas still comes from its threat to the environment. In addition, the policy of restricting the use of SF_6 in various countries gradually makes the study of alternative gases a hot issue in the global power industry.

Based on the above reasons, it has become an important research subject in the power industry to look for a new type of environmentally friendly gas with good insulation ability and safety. Research institutes across the world are dedicated to finding suitable gas alternatives to SF_6 for use in gas-insulated power equipment such as GISs and GILs.

III. EVALUATION INDICES OF ALTERNATIVE GASES

Alternative gases should be safe, harmless, and environmentally friendly and should meet the needs of equipment operation, such as the boiling point, insulation properties, interrupter performance, and decomposition characteristics. At present, the gas with alternative potential is mainly studied in terms of the insulation performance, the arc-extinguishing performance, and the decomposition characteristics. The summary of the research is shown in Fig. 2.

Based on the environmental parameter (GWP), insulation properties, safety, and other aspects, the main alternative gases and basic parameters are shown in Table II. The research focuses mainly on natural gases (N_2, CO_2, He, Ar, and so on), SF_6 gas mixtures, perfluorocarbons (c-C_4F_8, C_3F_8, and C_2F_6), CnFmX gases, and other gases such as HFOs.

A. Insulation performance

The macroscopic parameters of the insulation performance mainly include the breakdown voltage, the partial discharge (PD) inception voltage, and the volt-second characteristic of different gases tested, which can be measured in the test. The voltage type (DC, AC, or lightning impulse voltage), electric field uniformity, gas pressure, and mixing ratio of the insulated gas are all important factors to judge the insulation properties, as shown in Fig. 3. The experimental method of breakdown voltage is shown in Fig. 4. The measurement of partial discharge (PD) inception voltage needs to be combined with the voltage measurement device while measuring the impedance to collect the PD signals presented in the oscilloscope.

Among the influencing factors, the electric field uniformity is determined by the electrode structure, and the non-uniformity factor f of the electric field is given by

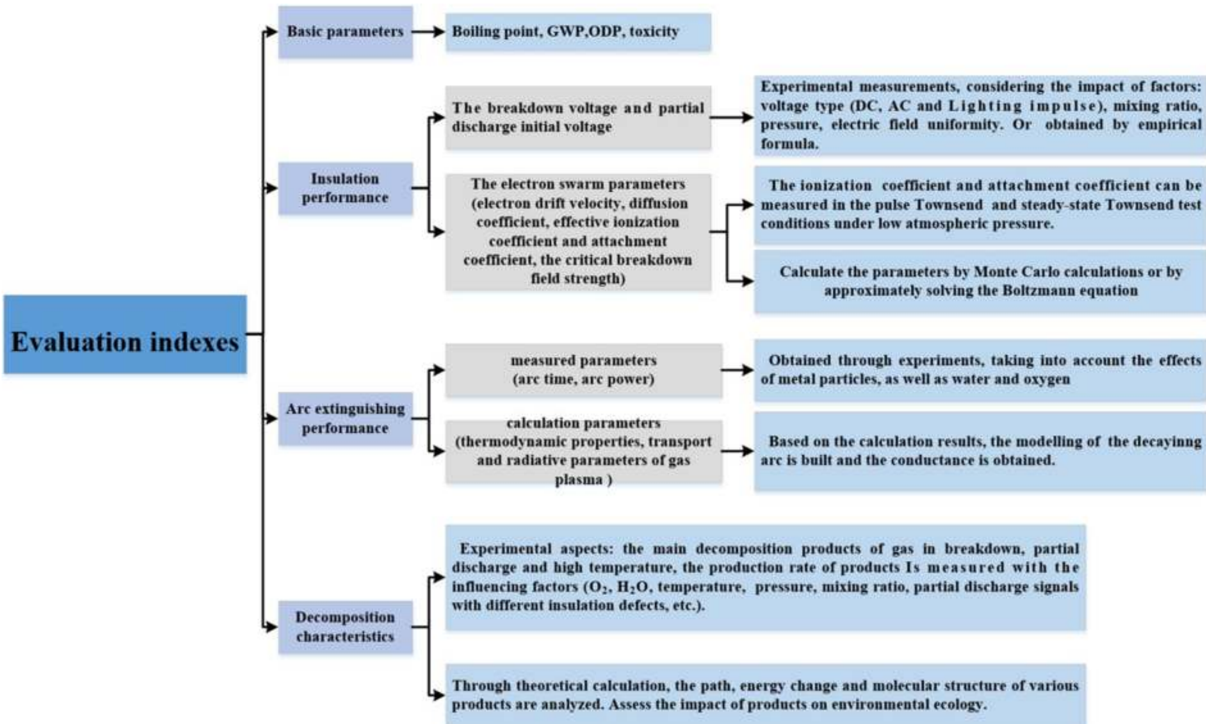

FIG. 2. Evaluation indices of alternative gases and research resource.

$$f = \frac{E_{max}}{E_{av}}. \tag{1}$$

In Eq. (1), E_{max} represents the maximum electric field strength and E_{av} represents the average electric field strength. The electric field distribution around the electrodes can be calculated by software such as COMSOL. Different gases have different sensitivities to electric field uniformity.

The influence of the gas mixture ratio on the insulation properties mainly refers to the synergistic effect of the mixed gases. When

TABLE II. Physical and environmental characteristics of common dielectric gases.[45–50]

Type	Insulation strength relative to SF_6	Boiling temperature (°C) (1 bar)	Lifetime (year)	GWP
SF_6	1	−63.9	3 200	23 500
N_2	0.36	−196	0	0
CO_2	0.30	−78.5	Infinity	1
Air	0.30	<183	Infinity	≈0
CF_4	0.39	−186.8	6 300	50 000
C_2F_6	0.78–0.79	−78	10 000	9 200
C_3F_8	0.96–0.97	−37	2 600	7 000
c-C_4F_8	1.25, 1.31	−6(-8)	3 200	8 700
CF_3I	1.23	−22.5	0.005	1–5
C_4F_7N	2.2	−4.7	0	2 100
$C_5F_{10}O$	2.0	27	0	1
$C_6F_{12}O$	2.5	49	0	1
CF_3NSF_2	2.41	−6	...	...
HFO1234zeE	0.98	−9	12	0.02
R12	0.9	−29.8	12	2 400

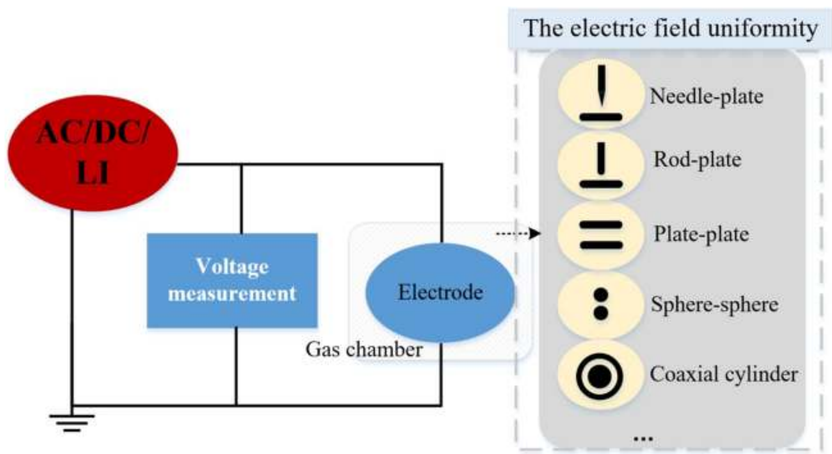

FIG. 3. Diagram of the breakdown voltage measurement.

two kinds of gases (at least one is a kind of gas with good insulation performance) are mixed, the insulation performance of the mixed gas shows three different variations with the increase in the insulating gas content: negative synergistic effect, linear relationship, and positive synergistic effect. Mixed gas with a negative synergistic effect is rare, which is not suitable as an insulating gas. The mixed gases with a positive synergistic effect will show great advantages such as the same insulating property as pure gas at a certain mixing ratio. Therefore, finding the characteristics of the synergistic effect is helpful to find the most suitable mixing ratio,

$$C = \frac{k(V_m - V_1)}{(1-k)(V_m - V_2)}, \tag{2}$$

where V_1 and V_2 are the breakdown voltage of the two pure gases 1 and 2 ($V_1 > V_2$) in kV, V_m is the breakdown voltage of the mixed gas in kV, k is the mixing ratio of gas 1, and C represents the degree of synergy of two gases. A smaller value of C indicates that the two gases have the better synergistic effect.[51] The basic synergy relationship of mixed gas: negative synergistic effect is shown in Fig. 4.

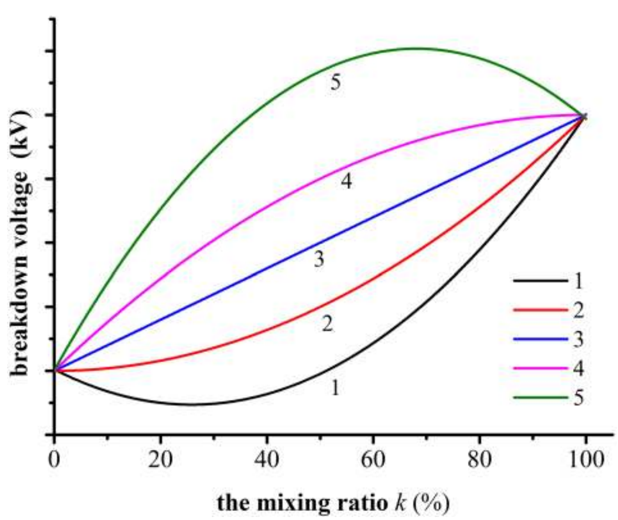

FIG. 4. Basic synergy relationship of mixed gas: negative synergistic effect $C > 1$ (curves 1 and 2), linear relationship $C = 1$ (curve 3), and positive synergistic effect $C < 1$ (curves 4 and 5).

The microscopic parameters for characterizing the gas insulation properties can also be measured experimentally or calculated theoretically. The experimental measurement process is shown in Fig. 5, which is generally performed under a steady-state Townsend (SST) test or a pulsed Townsend (PT) test (generally, the gas pressure is small at about 100 Pa).[52] The measured parameters include the effective ionization coefficient α of the molecule and the effective adhesion coefficient η. It is generally considered that the critical electric field E_{cr}/N can be obtained when the two coefficients are equal, which can be used as a reference value for measuring gas breakdown. According to Townsend discharge theory, α and η can be obtained by changing the electrode spacing d and measuring repeatedly current I, according to the following equation:

$$\boldsymbol{I} = I_0\left[\frac{\alpha}{\alpha-\eta}e^{(\alpha-\eta)\,\mathrm{d}} - \frac{\eta}{\alpha-\eta}\right]. \tag{3}$$

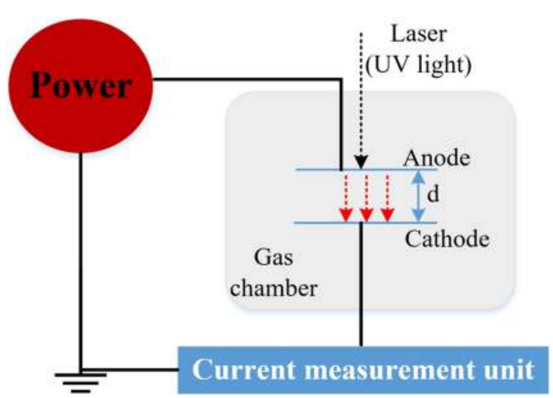

FIG. 5. Diagram of measuring microscopic parameters.

In theory, the electron swarm parameters (such as effective ionization coefficient, electron drift velocity, and particle diffusion coefficient) between gaseous molecules and electrons at the gas micro-level are theoretically calculated to comprehensively evaluate the insulating properties of the gas. The first step to obtain these parameters is the calculation of the collision cross section. More information about collisions in the main gases can be found in Ref. 53. There are two main methods of calculation: (1) the Monte Carlo simulation, which is the method with many iterations and computational complexity, and (2) solving the Boltzmann equation using some approximations. Indeed, the transport state and energy distribution of electrons in the discharge process should be clear. When the electron density is unevenly distributed, the electron diffuses from a high concentration point to a low concentration point, which is caused by the thermal motion of electrons. At the same time, under the action of the electric field, it accelerates the movement along the electric field to cause the collision ionization to form an electronic collapse. This complex state of motion results in different distributions of electron energy in the discharge space. In order to determine the transport state of charged particles, a self-consistent model need to be established that reflects the interaction between the electric field and the particles. In this complex model, both the elastic and the inelastic collision between electrons and gas molecules should be properly considered and the effect of the external electric field on charged particles should be taken into consideration. Therefore, some simplifications and approximations are usually needed to obtain electron swarm parameters and transport parameters during gas discharge. In a weakly ionized gas, the velocity distribution function $f(r, v, t)$ of electrons in a six-dimensional phase space obeys Boltzmann's equation,

$$\frac{\partial f}{\partial t} + v \cdot \nabla_r f + a \cdot \nabla_v f = C[f(r, v, t)], \tag{4}$$

where $a = eE/m$ is the acceleration of the electron under the action of an electric field, in which e and m denote the charge and mass of the electron, respectively. E is the electric field strength; v is the electron velocity; and r is the electron position parameter. $C[f(r, v, t)]$ refers to the collision process of electronic collision process, including the elastic collision and inelastic collision.

The general solution of Eq. (4) is obtained using the Legendre polynomial sphere expansion to construct a series of equations equivalent to Eq. (4) and to introduce the correlation coefficients. In the case of higher order expansion, it is usually necessary to introduce at least six parameters. However, for the second order, the equation can be greatly simplified,[54,55] but the corresponding assumptions need to be made.

(1) The distribution of the electric field in space is uniform.
(2) Collisions are stable over the mean free path dimension.
(3) The velocity distribution of the electron velocity distribution function $\boldsymbol{f}$ in the direction of the electric field is distributed symmetrically.
(4) In the time dimension, only the distribution of the electric field is considered stable and the electrons are in a state of stable distribution or high-frequency oscillation.

By assuming that the equation is simplified, the electron energy distribution function (EEDF) is obtained by approximately solving the Boltzmann equation, and the ionization coefficient and the attachment coefficient are obtained. When the ionization coefficient and the attachment coefficient are equal, the breakdown field strength is the critical breakdown field strength, (E/N)cr, and the parameters such as the electron drift speed and the average energy can also be obtained.[56,57]

In addition, some parameters are calculated based on quantum chemical calculation, such as the molecular ionization energy (IE), binding energy, surface area, and molecular polarization properties, and the gas insulation properties can also be predicted.[58]

B. Arc extinguishing performance

The main parameters for the experimental measurement are the gas arc time and the cut-off current value. Tests are generally carried out in the interrupter of the circuit breaker. According to Mayr's arc model,[59] the time constant and power loss coefficient of arc extinguishing can be obtained by changing the arc voltage (V) and arc current (I), based on the following formula:

$$\frac{1}{g}\frac{dg}{dt} = \frac{1}{\theta}\left\{\frac{Vi}{N_0} - 1\right\}, \tag{5}$$

where v is the arc voltage, i is the arc current, g is the arc conductance, θ is time constant, and N_0 is the power loss coefficient.

To judge the arc performance of the gas and finally to evaluate the arc extinguishing performance, the thermodynamic parameters and transport characteristics of the plasma formed during the arc process have to be determined depending on its thermodynamic state. When the temperature is very high, the plasma has a uniform thermodynamic temperature, and it is in a thermodynamic equilibrium state. At this point, the particle velocity is in accordance with the Maxwell–Boltzmann distribution, the population density of the ground state and excited state is in accordance with Boltzmann distribution, and the ionization process can be established based on the Saha equation. However, the complete thermodynamic equilibrium plasma can hardly exist in both natural and laboratory environments. For arc plasma, it is usually assumed that it is in the local thermodynamic equilibrium. Under this state, the particle collisions replace the radiation and occupy the dominant position in various reactions. The electron temperature is approximately equal to the temperature of heavy particles. The population density approximates the Boltzmann distribution, and the Saha equation is also approximately qualified. However, with the decrease in the arc temperature, the electron density decreases and the electron collisions gradually decay. The electron temperature deviates from the temperature of the heavy particles, and the arc plasma is in a non-thermodynamic equilibrium state. In addition, in the arc plasma, the rate of chemical reactions, such as decomposition, ionization, recombination, and adsorption, is limited. When the relaxation time of chemical reactions is less than the characteristic time of physical movement, such as particle convection and diffusion, the plasma reaches the local chemical equilibrium; otherwise, it is in the non-chemical equilibrium state.[60,61] In the study of non-chemical equilibrium, the speed of chemical reactions is the standard to judge the degree of chemical non-equilibrium. Therefore, the rate constant of chemical reactions becomes the key parameter to study the chemical reaction process. At present, an effective means of obtaining the reaction rate constant is by means of quantum chemical calculation.[62]

Due to the non-chemical equilibrium, the original statistical physics method cannot accurately describe the particle distribution and internal processes of the plasma. Instead, a control equation containing both the chemical reaction process and the physical process needs to be established for each particle so that the modeling and the computational difficulty are greatly increased. Most of the calculations are based on the local thermodynamic equilibrium and the two-temperature model under chemical equilibrium.[63] The calculation modeling is shown in Fig. 6. Under equilibrium conditions, there are two theories for the calculation of equilibrium compositions: one is based on the Saha equation and the Guldberg–Waage equation, combined with the Dalton partial pressure law, the conservation of chemical metrology and the conservation of charge to obtain the equilibrium compositions, and the other is solved by the minimum Gibbs free energy. Both of these computational theories are mathematically equivalent with all particles in the gaseous phase. The Saha equation is no longer applicable if the non-gaseous phase (e.g., solid, liquid, and molten) particles are considered, and the minimum Gibbs free energy method is applied. This method simplifies the modeling process without considering specific ionization and decomposition reactions, and it is widely used in the solution of equilibrium particle components.[64,65]

C. Decomposition characteristics

Insulation defects in the device can cause decomposition of the gas and further reaction with traces of impurities in the device to produce more complex products. The detection of discharge or high temperature decomposition products and the theoretical calculation of the decomposition process of mixed gas have also become an important issue in studying alternative gases. The decomposition characteristics are considered for the following reasons: First, the decomposition process and decomposition mechanism directly affect the gas self-recovery performance. Second, the products of decomposition, especially the gas and solid products that may be generated by breakdown, partial discharge, and electric arcs under different conditions, may have an impact on the environment and the safety of the human body. Finally, the decomposing characteristics of the alternative gas also provide a test method for the maintenance and operation after it has been applied to the equipment. The exploration of the decomposition process is also generally carried out through a combination of experiments and theoretical calculations. In the recent years, the influence of metal particles (such as Cu, Fe, and Ag), a small amount of gas impurities (such as H_2O and O_2), and temperature on the insulation properties has been deeply researched and explored. Even SF_6 decomposition has become an important diagnostic method for detecting SF_6 gas-insulated equipment. Under different insulation defects, SF_6 decomposition products showed different rules. The use of chemical means (GC-MS, infrared, UV, and nano-sensors) to detect these decomposition gases has also become an important study to determine the internal fault of the device and improve equipment maintenance.[66–78]

For the experiment, the gas in the chamber after the breakdown or partial discharge is collected and detected by the testing equipment such as the GC-MS or infrared spectrometer, as shown in Fig. 9. The main components of the decomposed gas can be obtained qualitatively or quantitatively. Generally, the

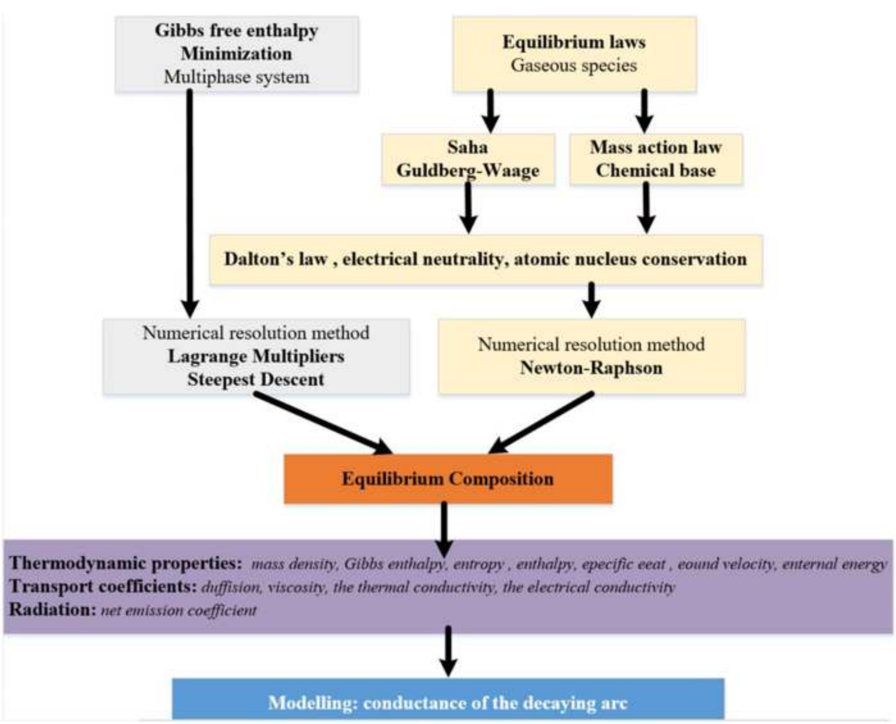

FIG. 6. Modeling of a decaying arc under local thermodynamic equilibrium.

FIG. 7. Measurement process of decomposition products.

possible products can be obtained through the qualitative analysis of the mass spectra or spectra, and then, the content of the products can be determined through the calibration of the standard gas. Through the XRD (x-ray diffraction) detection on the electrode surface, the atoms involved in the solid reaction can be clear during the gas decomposition process. The measurement process is shown in Fig. 7.[79]

In theoretical calculations, based on density functional theory (DFT), energy changes in chemical reactions, frequency characteristics, and transition state search, the basic properties of decomposition products are calculated by means of chemical molecular calculation software (Gaussian or Material Studio). In addition, using molecular dynamics in a constant temperature and constant volume system, we can calculate the decomposition process of gases at different temperatures to obtain the concentration of various free radicals. The reaction of gas molecules with H_2O or O_2 and the route of product generation are also important parts of the research.

TABLE III. Evaluation indices of alternative gases to have good properties.

Properties	Indices	Require values	Method
Insulation performance	Breakdown voltage	High	Measure
	Partial discharge inception voltage	High	Measure
	Synergistic effect	Low (less than 1)	Calculation based on the measured voltage
	Electron drift velocity	Low	Calculation
	Diffusion coefficient	Low	Calculation
	Effective ionization coefficient	Low	Calculation or measure
	Ionization coefficient	Low	Calculation or measure
	Attachment coefficient	High	Calculation or measure
	Critical electric field E_{cr}/N	High	Calculation
	Molecular ionization energy	High	Calculation or measure
Arc-extinguishing performance	Interrupting current	High	Measure
	Time constant of arc	Low	Measure
	Specific heat	High	Calculation
	Thermal conductivity	High	Calculation
	Electrical conductivity	Low	Calculation
	Net emission coefficient	Low	Calculation
	Conductance of the decaying arc	Low	Calculation
Decomposition characteristics	Toxicity of decomposition products	Low	...
	Formation rate of products	Low	Measure
	GWP and ODP of products	Low and 0	...

D. The main evaluation indices

The main evaluation indices of the insulation performance of gas-insulated media are shown in Table III, which may be helpful to evaluate the properties of new gases.

IV. THE RESEARCH RESULTS OF ALTERNATIVE GASES

A. Natural gases (N_2, CO_2, and air) and mixed gases

The natural gases with much lower liquefaction temperature and lower GWP than SF_6 have got relatively stable physical and chemical properties and are cheap. Therefore, it is better to use natural gases in gas-insulated equipment, especially in medium- and low-voltage equipment. Currently, natural gases used as insulating gases are N_2, CO_2, and air. Although the insulation performance is weaker than that of SF_6, these gases are initially considered as gases for insulation due to the simple molecular structure, and theoretical studies also started earlier. Until the introduction of alternative gases, these gases were focused and studied in more detail, both theoretically and experimentally. The related equipment is designed to produce and put into use. However, due to the relatively low insulation performance, it is necessary to take reasonable measures to improve the insulation properties such as increasing the gas pressure of the gas chamber, expanding the size of the equipment, and adopting the gas–solid insulation method.

1. Breakdown voltage

Husain and Nema[80] extended the Townsend breakdown formula to obtain Paschen curves for air, N_2, and SF_6, completing the evaluation of the three gas breakdown voltages. Hara *et al.*[81] studied the breakdown behavior of N_2 and N_2/O_2 gas mixtures in the presence of metallic particles at the solid–insulator interface of solid insulators. The effects of the cone insulator angle, particle size, and pressure were analyzed. Mizuno *et al.*[82] proposed a combination of the gas and solid insulation method. By wrapping rubber on the surface of the electrode, the breakdown voltage of N_2 can be increased by 1.5 times at 0.2 MPa, and the results can be used in gas-insulated switch devices. Philp[83] experimentally measured the breakdown voltage of the $N_2 + CO_2$ mixture in a ball grid electrode, which is only one-third that of SF_6.

Meijer *et al.*[84] compared the breakdown voltage of N_2 and CO_2 on the AC voltage of a plate electrode by experiments. Although the difference between the breakdown values of the two gases is not significant, CO_2 is more stable and the breakdown voltage of CO_2 linearly increases with the pressure value. In order to test the ability of the gas to withstand over-voltage in the field, Ueta *et al.*[85–87] tested the breakdown characteristics of CO_2 and N_2 under non-standard lightning impulse voltage and proposed a method to evaluate the performance of CO_2 gap insulation of non-standard lightning impulse waves. Pfeiffer and Schoen[88] experimented and studied the development of the streamer current before the breakdown of N_2 and N_2O mixed gases. It is believed that the use of the mixed gas in large-scale high-pressure equipment has obvious advantages. Pelletier *et al.*[89] measured the breakdown field strength of N_2 and He mixed gases under a uniform field and obtained the standard formula of the breakdown voltage and mixing ratio, Olivier's equation. Lim and Bae[90] studied the flashover voltage and the partial discharge inception voltage of dry air, N_2, O_2, and mixed gas on the surface of the GIS insulator. Considering economy and insulation performance, it shows that dry air is suitable for gas insulated switchgear.

Rokunohe *et al.*[91] found that the insulation property of air at 0.5 MPa is greater than that of pure N_2 and CO_2, and is comparable to that of N_2/O_2 (the mixing radio of O_2 is 20%). They pointed out that the dielectric strength of air at 0.6 MPa is 95% of SF_6/N_2 (the mixing radio of SF_6 is 5%). Pontiga found that N_2 and O_2 mixed gases produced N_2O under negative corona discharge.[92] Saitoh *et al.*[93] studied the partial discharge and breakdown characteristics of air and N_2 at the plate electrode. The partial discharge voltages of the two gases are almost the same, but the breakdown voltage of air is larger than pure N_2. Without changing the size of the equipment, using 1.0 MPa N_2 and solid insulation can replace 0.5 MPa SF_6.[94] Zhang *et al.*[95] proposed an improved design method of air gap and interface insulation. Based on the small or no SF_6 experiment in medium-pressure C-GIS, a low-pressure N_2 gas tank was used as the insulation gas to replace SF_6. A low-pressure N_2 gas tank 40.5 kV-1250 A three-phase C-GIS was developed. It has a vacuum interrupter and the same area covered as the SF_6 C-GIS.

2. Electron swarm parameters

Zhao *et al.*[96,97] calculated the critical breakdown field $(E/N)_{cr}$ of CO_2 mixed O_2 and H_2. Compared to pure CO_2 and 50% CO_2-50% H_2, the 50% CO_2-50% O_2 mixture has better breakdown characteristics. The $(E/N)_{cr}$ of the 50% CO_2-50% O_2 mixed gas almost does not change when the gas temperature is up to 2500 K. Although there is a significant decrease with the temperature rising to 3500 K, it is still higher than that of pure CO_2. Chen *et al.*[98] calculated the critical breakdown strength of CO_2 and mixed gases (CO_2, CO_2/O_2, CO_2/CH_4, CO_2/He, and CO_2/N_2) over a temperature range of 300 K–4000 K. The results show that the mixtures CO_2/O_2 and CO_2/CH_4 have a high critical breakdown field, which makes it possible to further improve the insulation properties of pure CO_2. Yousfi *et al.*[99] measured the electron swarm coefficients (drift velocity, diffusion coefficient, and effective ionization coefficient) of N_2, CO_2, and O_2, and mixed gases using a pulse Townsend discharge. The hindering effect of the two gases on the electrons was verified by solving the Boltzmann equation. Moruzzi and Price[100] measured the ionization coefficient of air in the range of 90-260Td. With the addition of a small amount of CO_2, the adsorption of air was significantly enhanced, but the electron attachment process of N_2 could not be detected. Raju and Gurumurthy[101] calculated the parameters of N_2 by solving the Boltzmann equation numerically. The electron average energy, drift velocity, and mean effective field intensity (E_{avef}) are obtained from the distribution function, and the field strength of the electron population is described when the electric and magnetic fields coexist. Kucukarpaci and Lucas[102] calculated the electron swarm parameters of CO_2 and N_2 over a large electric field (14–3000 Td) using the Monte Carlo algorithm using the latest collision cross section parameters, and the calculated results were consistent with the experimental measurements.

3. Interruption property

Stoller[103] tested the interrupting current of CO_2 as an interrupter medium in circuit breakers and calculated it by using a hydrodynamic model and found that the thermal disruption performance of CO_2 is lower than that of SF_6 but higher than air. Optimizing the circuit breaker structure may result in the CO_2 substitution of SF_6 as an arc extinguishing medium. Jonsson *et al.*[104–107] tested the ability of air to break in a 630 A/24 KV medium voltage load short-circuit switch. Optimization of the contact and nozzle structure helps improve the ability to interrupt, while the length and diameter of the nozzle have little effect on the ability to interrupt. Uchii *et al.*[108] tested the ability of CO_2 to break off in a GCB (gas circuit breaker). At the same gas pressure, the thermal shutdown capacity of CO_2 is about 50% of SF_6. By blowing more heat through the improved mixing chamber, the cut-off capacity of CO_2 can be increased by 30%.

Chen *et al.*[109,110] established the arc model to simulate the interruption ability of the vacuum-CO_2 mixed circuit, and the results show that with the combination of vacuum interrupters, the current interruption capacity of CO_2 gas can be increased. Matsumura *et al.*[111] studied the current interruption ability of CO_2 mixed with N_2, O_2, He, and air. It was found that the conductance of the residual arc of the CO_2 mixture of O_2 or He (the mixing ratio of CO_2 is 20%) decreased more rapidly and the breaking capacity improved significantly. In theoretical calculation, Zhong *et al.*[112] studied the thermal physical properties of plasma and the effect of the copper vapor from the electrode surface of the circuit breaker on the CO_2–N_2 mixture. The behavior of gas during the quenching process was analyzed based on the thermodynamic parameters and transport characteristics. The existence of copper vapor in the equipment was also analyzed. The influence of copper vapor on the thermodynamic properties of the mixed gas was evidently influenced by the ionization properties of the copper atom itself, atomic density, as well as partition function.

The advantages of natural gas are low cost, harmless to the environment, and no security threat to ecology and human resources. At present, there are already finished products in middle and low voltage equipment (ABB, Schneider, and other companies) using conventional gas as an insulation medium. The main properties are shown in Table V of the Appendix. CO_2 is likely to be used as an arc extinguishing medium in circuit breakers. The use of conventional gas in the switch equipment needs to optimize the structure of the equipment reasonably, and the mechanical structure and electrical performance have greater space to improve. Simply relying on increasing the pressure and increasing the size will reduce the safety of the equipment and increase the production cost of the equipment. It is also an effective means to use the solid insulation material. However, solid insulation materials exist in the atmosphere for a long time and are difficult to degrade. Adding solid insulation materials to the equipment will undoubtedly increase the environmental burden on the other hand. However, this kind of gas still has a great prospect of development and use, which has a great exploration value.

B. Mixtures of SF_6 with natural gases

Although the study of the SF_6 gas mixture started earlier, there is no interruption in the exploration of insulation and arc extinguishing ability. At this stage, research focuses more on practicality. The SF_6 gas mixture, which generally refers to the mixture of SF_6 and some buffer gas with relatively poor insulation and a very low boiling point (air, N_2, CO_2, N_2O, CF_4, H_2, and some inert gases), not only meets the equipment insulation requirements but also reduces the amount of SF_6.

1. Breakdown voltage

Malik and Qureshi[113,114] compared the breakdown voltage of SF_6 mixed with N_2, CO_2, and air. It was considered that SF_6 mixed N_2 was the most ideal mixed gas. The mixture is non-toxic and non-flammable, and when the SF_6 mixing ratio reaches 50%–60%, the insulation performance can reach 85%–90% of the pure SF_6. When the lightning impulse voltage was applied, the addition of a small amount of SF_6 to N_2 increased the positive lightning impulse breakdown voltage of N_2. This is due to the positive space charge resulting in an anode shield.[115] Farish *et al.*[116] investigated the effect of the surface roughness of the SF_6 and N_2 mixed gas on the breakdown voltage with a coaxial electrode. Compared with pure SF_6, the mixed gas is not sensitive to the electric field roughness. Graf and Boeck[117] studied the sensitivity of the SF_6/N_2 mixed gas to non-uniform electric fields by setting protrusions on the electrodes. The mixed gas is more sensitive to non-uniform fields than SF_6 at the same dielectric strength. Woo *et al.*[118] measured the breakdown performance of the SF_6/N_2 mixture at the lightning impulse voltage and AC voltage. As the electric field uniformity increased, the slope of the breakdown voltage decreased. In the lightning impulse test, the positive breakdown voltage was higher than the negative breakdown voltage. Guerroui and Lemzadmi[119] by experiment measured the initial partial discharge voltage of the SF_6 and N_2 mixed gas under a non-uniform field. The initial voltage increases with an increase in pressure, and the positive polarity was higher than the negative polarity. Sato *et al.*[120] designed a gas insulated bus with SF_6/N_2 as gas-insulation. Compared with 0.4 MPa pure SF_6 gas insulated busbars, if a 0.6 MPa 10%SF_6-90% N_2 mixed gas is used, the diameter of the tank needed to be increased by 15%. Hoshina *et al.*[121] tested the insulation properties of the SF_6/N_2 mixture on a full-scale gas-insulated busbar model and analyzed the effect of contaminated particles on the breakdown characteristics of AC voltage and impulse voltage. The mixed gas at 0.3 MPa and 0.5 MPa showed a positive synergistic effect, and the partial discharge inception voltage of the mixed gas showed a negative synergistic effect. Guo *et al.*[122] studied the lightning impulse breakdown voltage of the SF_6/N_2 mixture, which showed a negative synergistic effect at low gas pressure. Rizk and Eteiba[123] measured the breakdown voltage and time of a mixture of SF_6 and N_2 under the coaxial electrode and validated it theoretically. Mizobuchi *et al.*[124] observed the streamer development of SF_6–N_2 mixed gas discharge by experimental tests and verified by numerical calculation. The electric field was kept constant during the development of the streamer by single steep square high voltages in the measurements. At different mixing ratios, the development trend of the flow-injection process was similar. Jiasen *et al.*[125] tested multi-channel discharge characteristics of SF_6–N_2 or SF_6–Ar gas with different mixing ratios in a coaxial distorted electric field using 40 kV–78 kV pulse power. The results showed that the discharge channels of the SF_6–Ar or SF_6–N_2 mixture decreased with the increase in the SF_6 mixing ratio and then tended to be saturated. Hirata *et al.*[126] tested the creeping discharge characteristics of the mixed gas. The flashover voltage of 3% SF_6 mixture was lowest with a positive polarity impulse voltage. The mixtures of SF_6 and N_2 gases have been used in GIL. The first GIL that used the SF_6/N_2 gas mixture as the insulation medium developed by Siemens was put into operation at Geneva International Airport in Switzerland in 2001.[127] Currently, the SF_6/N_2 gas mixture GIL has been successfully applied in the 245 kV–550 kV line.

The SF_6-air mixture has a more stable corona for positive DC voltages.[128] Li *et al.*[129] measured the breakdown characteristics of the gap between coaxial electrodes of various impulse power sources for SF_6 (1%) with air and N_2 gas mixtures in the range of 100 kPa–500 kPa. The results showed that the influence of the waveform on the breakdown voltage was great. Under the coaxial electrode, little change was caused in insulation properties with adding 1% of the SF_6 in the air, which is different from the situation under a non-uniform field.

Qiu *et al.*[130–132] compared the dielectric properties of SF_6/N_2 and SF_6/CO_2 mixtures and concluded that the dielectric properties of the SF_6/N_2 mixed gas are better than that of SF_6/CO_2 in uniform or quasi-uniform fields, but SF_6/CO_2 on the contrary is better than SF_6/N_2 under the non-uniform fields. By testing the breakdown voltage of 50% SF_6 mixed CO_2 and N_2 at 60 Hz alternating current, it was found that adding a small amount of CO_2 into the 50% SF_6/N_2 mixture can significantly improve the breakdown voltage. The breakdown voltage of 50% SF_6-49% N_2-1% CO_2 is 1.35 times that of 50% SF_6-50% N_2 and 1.15 times that of pure SF_6.[133] By testing the breakdown behavior of mixed gases under the rod-plate electrode, it was found that the breakdown voltages of SF_6–N_2 and SF_6–air were similar under the negative impulse voltage.[134] The SF_6–CO_2 breakdown voltage is higher than the other two. As the gas pressure is higher than 0.1 MPa, the three kinds of mixed gases produced a leader before the breakdown. With the increase in the SF_6 mixing ratio and pressure, the leader showed a gradual development.

Cookson and Wootton[135] tested the corona and breakdown voltage at AC voltage with a mixture of SF_6 and H_2. The addition of a very small amount of SF_6 (0.002%) to H_2 increases the breakdown voltage of pure H_2 by 70%. The starting voltage of pure SF_6 is about 2.7–3 times that of pure H_2. Adding a small amount of SF_6 (within 1%) to H_2 does not affect the corona onset voltage. Farish *et al.*[136] tested the breakdown voltage of the SF_6 and H_2 mixed gas at negative polarity lightning impulse voltage. For H_2, the breakdown voltage of the negative lightning impulse is 60%–100% higher than that of the positive polarity. However, adding a small amount of SF_6 (within 1%) to H_2 increases the rate of increase in breakdown voltage less than the positive polarity.

Akbar and Malik[137] measured the breakdown voltage of several mixed gases at DC voltage. The measurement results showed that the mixed gas containing N_2O was less sensitive to electrode surface defects. Park *et al.*[138,139] tested SF_6/CF_4 mixed gas insulation performance, including the lightning impulse test, AC frequency test, and partial discharge test in a 25.8 kV three-phase GIS tank. The experimental results showed that the breakdown voltage increased with the SF_6 content, which showed that the mixing ratio of SF_6 had little effect on the starting voltage. Berg *et al.*[140–142] studied the insulation properties of SF_6 and CF_4 gas mixtures at DC voltage, 60 Hz AC voltage, and standard lightning impulse voltage. The SF_6 and CF_4 mixed gas was more suitable than the SF_6–N_2 mixed gas to be used as an arc extinguishing medium. Lee *et al.*[143] compared the breakdown characteristics of N_2, SF_6, and CF_4 in high-voltage bushing at low temperatures. Due to its outstanding insulating properties and low boiling point, CF_4 has shown its obvious superiority in cold environments.

Siddagangappa *et al.*[144] proposed a simple calculation formula to predict the breakdown voltage of SF_6 and mixed gases under a uniform electric field. Nema *et al.*[145] proposed a breakdown voltage calculation formula of the SF_6 mixed gas under a uniform and non-uniform electric field, which was used to infer the insulating properties of the mixed gas. The calculation results were consistent with the experimental test results. The limitation of the formula is that the parameters in different gas formulas are different and not universal.

2. Electron swarm coefficients

Maller and Naidu[146] measured the ionization and attachment coefficients of the SF_6 mixed air and nitrogen. In the meantime, using the calculation method, the breakdown field strength of the three mixed gases of SF_6–N_2, SF_6–air, and SF_6–CO_2 was calculated in the pressure range from 100 kPa to 500 kPa, and the insulation properties were predicted.[147] Govinda Raju calculated the breakdown field strengths of SF_6/N_2 and SF_6/N_2O mixed gases by solving Boltzmann parameters.[148] Kline *et al.*[149] calculated the electron swarm parameters of SF_6 mixed with He and N_2. The critical breakdown field strength of the mixed gas was obtained from the ionization coefficient and the attachment coefficient. Dincer and Govinda Raju[150] measured the ionization and attachment coefficients of SF_6 and N_2 mixed gases at steady state Townsend discharge. Govinda Raju *et al.*[151] used the steady-state Townsend apparatus to measure the ionization of the SF_6 and N_2 mixed gas and obtained the critical breakdown field strength of the mixed gas. The breakdown field strength does not show a simple linear relationship with the increase in the SF_6 content, and a synergistic effect existed. Lee[152] measured the relative parameters of a mixture of SF_6 and CO_2. Fréchette[153] used the SST apparatus to measure the ionization coefficients of the SF_6/N_2 and $SF_6/CC_{l2}F_2$ mixed gas to obtain the limited breakdown field strength. For the SF_6/CCl_2F_2 mixed gas, the ionization coefficient was not linear with the SF_6 mixing ratio, and there was a synergistic effect. The breakdown strength of the mixed gas with a SF_6 mixing ratio of 25% was 5% higher than that of pure CCl_2F_2. Using the latest collision cross section data, Phelps and Van Brunt[154] calculated the electron swarm parameters (transport, ionization, adhesion, and diffusion coefficients) of SF_6 and N_2, O_2, and He mixtures by solving two Boltzmann equations approximately. The electron swarm process of the SF_6 and CO_2 mixture under PT discharge was calculated, as well as the ionization, adsorption, and dissociation coefficients.[155] Adding a small amount (2%–5%) of SF_6 into CO_2 under the condition of pulsed Townsend discharge has no obvious effect on the electron drift speed and diffusion coefficient function. However, it had a significant impact on the effective ionization process. Under the same mixing ratio, the critical breakdown strength of SF_6–CO_2 was lower than that of SF_6–N_2.[156] Urquijo measured the electron drift, diffusion, and effective ionization processes and attachment coefficients for SF_6/CHF_3 and SF_6–CF_4 mixed gases under PT discharge conditions. The electron drift and diffusion process had no relation with the SF_6 content, but the ionization coefficient depends on the SF_6 content. The critical breakdown fields of both gases were lower than SF_6–N_2.[157] Xiao *et al.*[158] and Liu and Xiao[159] calculated the electron swarm parameters of SF_6 and CF_4 using the Monte Carlo method. With the increase in the SF_6 content, the breakdown voltage increased the effective ionization coefficient decreased. The electron diffusion coefficient of CF_4 was larger than SF_6. The improved Monte Carlo algorithm was used to calculate the electron swarm parameters of the SF_6/N_2 mixed gas, and the calculation was further improved.[160] Zhao *et al.*[161] calculated the critical breakdown field strength of mixed gas of 0.01–1.6 MPa SF_6 and N_2 with the temperature of 300–3000 K. The minimum Gibbs free energy was used to calculate the equilibrium composition of particles. The electron energy distribution function was obtained using various particle data analyzed by the Boltzmann equation. At higher gas temperatures, the addition of N_2 to SF_6 gas reduced the kinetic energy of the electrons and increased the breakdown field strength. Increasing the N_2 concentration effectively increased the $(E/N)_{cr}$ of SF_6–N_2 mixtures at gas temperatures around 2000–3000 K. The same method was used to calculate the SF_6–CF_4 gas mixture. At low temperatures, the breakdown field of pure SF_6 was higher than that of the mixed gas, but the breakdown strength of the mixed gas was higher than that of SF_6 at temperatures greater than 4000 K (0.4 MPa).[162] For the SF_6–CO_2 mixed gas, a large amount of CO_2 could reduce the number of high-energy electrons. When the temperature was higher than 1740 K, the addition of CO_2 to SF_6 could improve the insulation performance. However, adding too much CO_2 at low temperatures may cause the insulation performance to decrease. At 0.8 MPa, the dielectric properties of the mixed gas increased with an increase in pressure.[163] Larin discussed the synergistic effect of SF_6/CF_4 gas mixtures based on solving the Boltzmann equation.[164]

3. The interruption performance

Lee and Frost[165] studied the interruption ability of SF_6 and its mixed gas and evaluated the arc extinguishing performance of 15 gases and mixed gas at 60 Hz AC. It was showed that the arc extinguishing performance of these gases and mixed gases was lower than that of pure SF_6. Tomita *et al.*[166] studied the interruption capability of 20% SF_6 and 80% Ar mixed gas in circuit breakers. The development of arc quenching was analyzed, and the electron density was measured. The arc extinguishing speed of mixed gas was faster than that of pure Ar. Gleizes *et al.*[167] calculated the transport parameters of the SF_6 and N_2 mixed gas plasma at temperatures from 1000 K to 15 000 K. With the temperature below 8000 K, the conductivity of the 50% SF_6–N_2 mixed gas was similar to SF_6, and much larger than pure N_2, which was due to the lower ionization coefficient of the S atom. At temperatures greater than 4000 K, the thermal conductivity of the mixed gas was greater than that of pure SF_6. In order to evaluate the arc-extinguishing ability of SF_6-CF_4 and SF_6–C_2F_6 mixed gas, Chervy *et al.*[168,169] calculated the main parameters of the plasma based on the local thermodynamic equilibrium, which mainly referred to the thermodynamic parameters and transport parameters. The arc-extinguishing performance of SF_6–CF_4 and SF_6–C_2F_6 mixed gases was better than that of SF_6–N_2, and SF_6–CF_4 was superior to SF_6–C_2F_6. The thermodynamic properties of CF_4 with a better ability to interrupt were more stable than those of C_2F_6. When the mixing ratio of SF_6 exceeded 50%, the interruption performance of the mixed gas approached SF_6. With the mixing ratio of SF_6 below 25%, the performance is close to CF_4. 40% SF_6 mixed with CF_4 is a more appropriate mixing ratio. The arc extinguishing performance of the SF_6–CO_2 mixture used in circuit breakers was evaluated by calculating the mixed gas transport parameters (thermal conductivity and conductivity).[170] Wang *et al.*[171] calculated the effective ionization coefficient and the critical breakdown field strength of the SF_6 and He mixed gas at a high temperature (300 K–3500 K) in a high voltage circuit breaker. The mixed gas showed better interruption ability because of the He with a higher ratio thermal and thermal conductivity. CF_4 also had a good arc-extinguishing performance to be used in equipment such as a 115 kV/40 kA high voltage circuit breaker with 50%SF_6/50%CF_4 at 0.7 MPa gas pressure applied in the Manitoba hydropower station of Canada. SF_6/CF_4 circuit breakers with a rated voltage of 550 kV, a nominal current of 4 kA, and a breaking capacity of 40 kA operated at the Dorsey Converter Station.[172] In the plasma calculation, Yang *et al.*[173,174] calculated the thermodynamic properties and transport parameters of the plasma of SF_6 mixed with N_2 and CO_2 at high temperatures, as well as the influence of metal particles. In the non-thermodynamic equilibrium, the plasma behavior has been analyzed and discussed. Under the non-thermodynamic equilibrium condition, the difference of the conductivity between the mixed gas and N_2 was larger. The thermal conductivity of mixed gases also appeared significantly different, especially below 2000 K.

4. Decomposition characteristics

Pradayrol *et al.*[175] examined the major decomposition products of 50%SF_6 mixed 50%CF_4 at 50 Hz AC, including SOF_2 + SF_4, SOF_4, SO_2F_2, S_2F_{10}, S_2OF_{10}, $S_2O_2F_{10}$, and $S_2O_3F_6$. The addition of CF_4 to SF_6 had little effect on the major decomposition products. When H_2O and O_2 were present, the formation of the major products (SF_4 + SOF_2) and S_2F_{10} was reduced. In the presence of solid insulation, the products of the mixed gases were similar to pure SF_6. When H_2O, O_2, and insulators exist, they can interfere with each other.[176] Under negative corona discharge, O_2 and H_2O (less than 0.2% H_2O and less than 1% O_2) enhanced the production of all sulfur oxyfluoride. At lower pressures, product generation increased. The presence of 50%CF_4 inhibited the production of all compounds.[177] SF_6/O_2 under spark discharge decomposed SOF_4, SO_2F_2, SOF_2, and SO_2.[178] The main products of SF_6 and N_2 included SOF_4, SO_2F_2, SF_4 + SOF_2, SO_2, S_2OF_{10}, S_2F_{10}, $S_2O_2F_{10}$, $S_2O_3F_6$, SF_5NF_2, NF_3, and $(SF_5)_2NF$ during AC corona discharge. Adding a small amount of water molecules would affect the rate of formation of all products. The production of SF_5NF_2, NF_3, and $(SF_5)_2NF$ was minimal compared to other products. N_2O and CO_2 were also produced at higher pressures.[179,180] SF_6 and N_2 produce the same decomposition when AC spark discharges.[181] When a small amount of CO_2 was added to the mixture of SF_6 and N_2, the generation of SOF_4 + SO_2F_2, COF_2, CO, and S_2F_{10} was reduced under negative DC corona.[182] Since SF_6 and N_2 have been used in the GIL, their decomposition products in the case of partial discharges and their discharge characteristics were helpful for the detection of partial discharges and insulation monitoring. However, the decomposition products of mixed gases are more complicated than pure SF_6, and the difficulty in insulation monitoring is further increased.

Mixed gases are suitable for equipment in extremely cold areas, such as northern China. However, the recycling and reuse of mixed gases still need to be improved and optimized for existing SF_6 equipment.[183,184] ABB proposed a standard for the use of SF_6 gas mixtures in equipment, proposing that the assessment of the environmental

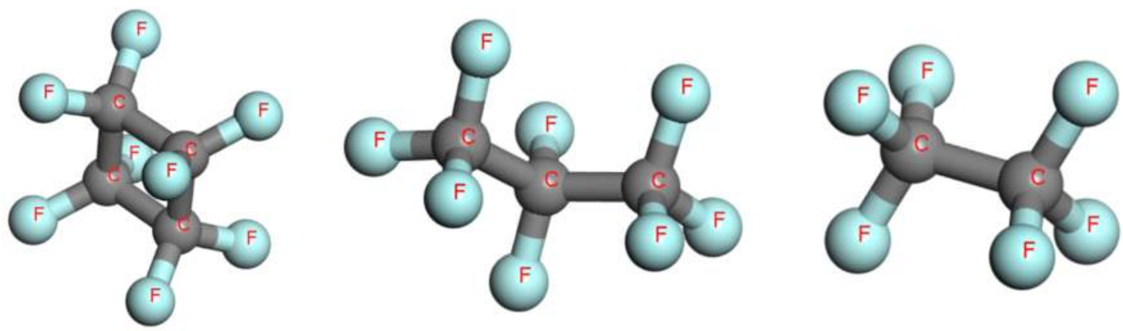

FIG. 8. PFC molecular structures.

impact needs to take into account the time period. The mixed gas should be reused in the field without generating other gas components and be easy to recycle separation. The existing SF_6 recovery equipment needs to be rebuilt and upgraded to recover the mixed gas.[185]

The use of SF_6 gas mixtures in electrical equipment has the obvious advantage of lowering the boiling point and maintaining good insulation properties. The main properties of SF_6 mixtures are shown in Table VI of the Appendix.

C. Mixtures of perfluorocarbons (PFCs) with natural gases

In order to completely replace SF_6, some electronegative gases with a low greenhouse effect and reliable insulation have become the main research objects. Compared with SF_6, the PFCs have better insulating properties and the GWP value is lower relative to SF_6. The typical electronegative gases studied today are c-C_4F_8, C_3F_8, C_2F_6, and CF_4 based on the boiling point, safety, and insulation properties. The molecular structures are shown in Fig. 8. The insulating gas and the buffer gas are generally mixed (N_2, CO_2, etc.), which reduces the gas cost and lowers the boiling point of the mixed gas under the premise of ensuring the dielectric strength.

Takuma *et al.*[186] calculated the boiling point of the mixed gas as a function of the mixing ratio according to the van der Waals formula and tested the breakdown voltage of the mixed gas of c-C_4F_8 and N_2. The insulation performance of the c-C_4F_8 gas under a uniform electric field is 1.18–1.25 times that of the SF_6 gas. Although the price of c-C_4F_8 is ten times that of SF_6, the actual usage is much smaller than that of SF_6. The use of c-C_4F_8 as an arc-extinguishing medium may produce carbon particles that affect the insulation properties. Adding a buffer gas such as CO_2 and N_2 can ease the formation of particles. Wada *et al.*[187] tested the breakdown behavior of the four perfluorocarbon gases, c-C_4F_8, l-C_3F_6, C_3F_8, and C_2F_6, under AC voltage at the plate–plate electrode and combined them with CO_2, N_2, and CF_4, respectively. It was found that PFCs and buffer gas mixtures have shown a positive synergistic effect. At the same time, the gas mixture was analyzed in terms of the boiling point and GWP. When the ambient temperature is above −20 °C, the insulation performance of the mixed gas can reach 70% that of SF_6 and the GWP is reduced by 30%.

Zhao *et al.*[188] studied the synergistic effect of the c-C_4F_8/N_2 mixed gas at lightning impulse voltage. The effect of gas pressure on the synergistic effect is not significant, and the obvious polar effect appears in the discharge characteristic of c-C_4F_8/N_2. The breakdown voltage under negative impulse was lower than that under positive impulse. This was because the polarity of the lightning impulses affects the speed and kinetic energy of free electrons. The free electrons in a negative lightning strike had a higher velocity, making the c-C_4F_8 to absorb fewer free electrons, so the breakdown voltage under negative lightning impulses was lower than the breakdown voltage under positive impulses.

Whitman[189] studied the impulse breakdown characteristics of C_3F_8 and compared it to air. At both positive and negative impulse voltages, the breakdown voltage of C_3F_8 was about 2.5 times that of air with both electrodes (ball and plate electrodes). Okubo *et al.*[190] tested the partial discharge inception voltage and breakdown voltages of C_3F_8 and C_2F_6 with the needle plate electrode. The synergistic effect of the C_3F_8/N_2 and C_2F_6/N_2 mixed gases was lower than that of SF_6/N_2. The breakdown voltage of the mixed gas is arranged in descending order of SF_6/N_2, C_3F_8/N_2, and C_2F_6/N_2.

de Urquijo and Basurto[191] used the PT test to measure the C–C_4F_8 electronic parameters such as the ionization coefficient, attachment coefficient, and diffusion coefficient, resulting in a critical breakdown field strength of 439.5 Td (1 Townsend = 10^{-17} Vcm^2), which is larger than that of SF_6 (369Td). Itoh *et al.*[192] calculated the electron transport parameters of the mixed gas of SF_6 and c-C_4F_8. The insulation characteristics of the mixed gas are better than that of pure gases. Wu *et al.*[193] and Liu *et al.*[194] calculated the critical breakdown field strength of the mixed gases of c-C_4F_8 and N_2 under pulsed discharges using Monte Carlo. The calculated results showed that the insulating properties of the mixed gases of c-C_4F_8 and N_2 were comparable to those of the SF_6/N_2 mixed gas, but the GWP value decreased significantly. Liu calculated the insulation properties of the mixed gas of c-C_4F_8 and CO_2 in the same way. As a result, the critical breakdown strength of the mixed gas of c-C_4F_8 and CO_2 was greater than that of the mixed gas with SF_6/CO_2. Li *et al.*[195] calculated electronic swarm parameters of the c-C_4F_8 mixed gas The critical breakdown field strength of c-C_4F_8–N_2 and c–air were similar and significantly higher than other mixed gases. The insulation performance of C_4F_8 can reach levels of pure SF_6 when the content exceeds 80%. Deng *et al.*[196] used the same calculation method to analyze the insulation properties of C_3F_8 mixed N_2 and CO_2. Under the same mixing ratio, the critical breakdown strength of the C_3F_8–N_2 gas mixture is greater than that of C_3F_8–CO_2. The C_3F_8–N_2 gas mixture containing 20% C_3F_8 can reach 60% of the dielectric strength of pure C_3F_8. Xiaoling *et al.*[197] proposed a method for evaluating the electronegativity of a gas by calculating the electron transport parameters of the molecule. The electron attachment property of the molecule was obtained by the Boltzmann equation under steady state Thomson discharge. It was found that the ability of c-C_4F_8 to attach electrons was still weaker than that of SF_6 and its electronegativity coefficient was at least three orders of magnitude lower than that of SF_6.

Koch and Franck[198] studied the characteristics of the C_3F_8 gas during partial discharge and breakdown. It is found that the discharge characteristics of the SF_6 gas were approximately similar from the results of discharge capacity, flow propagation time, and time interval, which may be related to $(E/N)_{cr}$, and ionization coefficients were closely related. The same model was used to predict the breakdown voltage and PD voltage of the CF_4 gas.[199] By calculating the breakdown parameters of C_3F_8–CF_4, C_3F_8–CO_2, C_3F_8–N_2, C_3F_8–O_2, and C_3F_8–Ar of C_3F_8 in the temperature range 300–3500 K, Wang *et al.*[200] found that the ionization coefficient of C_3F_8–N_2 was higher, and the attachment coefficient of C_3F_8-CF_4 was the largest. Under a normal temperature, the insulation property of C_3F_8/N_2 was outstanding. However, the critical breakdown strength of C_3F_8 decreased with the increase in temperature. The same method was used to calculate the critical breakdown field of the CF_4 plasma and predict the insulating properties.[201]

Lisovskiy *et al.*[202] measured the DC breakdown voltage of CF_4 at low pressure and calculated the electron swarm parameter of the gas at a small PL value (PL < 2 Torr cm, where P is pressure and L is distance). Wang *et al.*[203,204] calculated the thermodynamic parameters and transport parameters of the main PFCs (CF_4, C_2F_6, and C_3F_8) in the temperature range of 300–30 000 K, including the electron diffusion coefficient, viscosity, thermal conductivity, and conductivity, extending to the third order approximate (viscosity of the second order) Chapman–Enskog method. Theoretical calculations were made to analyze the arc-extinguishing properties of the three gases. The thermodynamic properties of olefinic gases (C_2F_2, C_2F_4, C_3F_6, etc.) containing C=F double bonds were also analyzed.

Kang *et al.*[205] studied the decomposition products of c-C_4F_8 and mixed gas with N_2 at 50 Hz AC corona discharge. The products of pure c-C_4F_8 gas discharge mainly included CF_4, C_2F_4, C_3F_6, C_2F_6, and C_3F_8, and C_2F_3N was produced in the mixed gas.

The insulation properties of c-C_4F_8, C_3F_8, and C_2F_6 all reach or exceed the level of SF_6, and the GWP values are obviously smaller than those of SF_6 (8700, 7000, and 9200, respectively). However, due to the limitation of the boiling point, it is necessary to mix with the buffer gas. With the addition of the buffer gas, the environmental impact obviously decreases, and the insulating property of the mixed gas also decreases. The main properties of PFCs mixtures are shown in Table VII of the Appendix. There is no obvious advantage in dielectric strength, which restricts the research and exploration process.

D. C_nF_mX mixtures

1. Mixtures of CF_3I with natural gases

One of the F atoms in CF_4 is replaced by the iodine atom from the CF_3I molecule, as shown in Fig. 9, and the performance of the molecule is greatly changed. Initially, CF_3I was considered as an alternative to the Halon 1301 fire extinguishing agent because CF_3I has no effect on the environment and is non-flammable and non-explosive.[206,207]

The initial study found that the CF_3I gas has good electron attachment capacity. The calculation of the electron swarm parameter showed that the critical breakdown field strength was higher and even higher than SF_6. From 2010, one after another, researchers began to explore the possibility to apply it in electrical equipment.

The AC breakdown voltage of the CF_3I/N_2 mixed gas in the non-uniform field was investigated, and the effects of pressure, electrode spacing, and mixing ratio were analyzed. When the mixing ratio was 30%, the breakdown voltage of the CF_3I/N_2 mixture was about 85%–90% of that of SF_6 at a pressure of 0.3 MPa, but the cost of gas was three times higher than the SF_6 one.[208] At the same time, the initial voltage of partial discharge of the CF_3I/CO_2 mixed gas was measured. The partial discharge initial voltage of the CF_3I/CO_2 mixed gas is 0.9–1.1 times that of SF_6/CO_2. The PD performance of the CF_3I/CO_2 mixed gas, with a CF_3I volume fraction of 30%–70%, was about 0.74 times of that of pure SF_6. The CF_3I/CO_2 mixed gas showed a good synergistic effect, with a value of 0.53.[209]

Toyota *et al.*[210] used square pulse voltage as a transient overvoltage to detect the (V-t characteristic) relationship between the breakdown voltage and the breakdown time of the CF_3I–N_2 and CF_3I–air mixture at the plate electrode. The test results showed that the breakdown voltage of pure CF_3I was 1.2 times that of SF_6 at the same pressure. The breakdown voltage of the CF_3I–N_2 and CF_3I–air mixture increased with the increase in the CF_3I mixing ratio. When the mixing ratio of CF_3I reached 60%, the dielectric strength of the mixed gas can reach the level of pure SF_6.

Yuan *et al.*[211] measured the gas–liquid equilibrium data (CF_3I + CO_2) at 243.150 K. The experimental data were modified by Peng–Robinson (PR) on the classical van der Waals formula to get the rule that the vapor pressure of the CF_3I and CO_2 gas mixture and its mole fraction change with the operating environment of GIS/GIL.

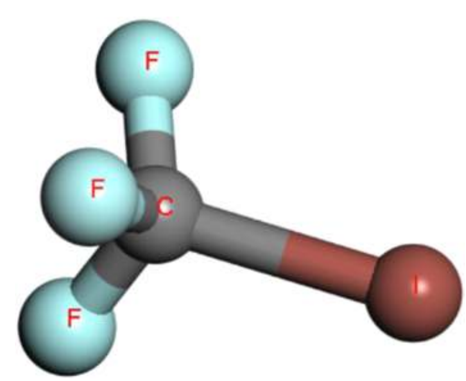

FIG. 9. Molecular structure of CF_3I.

Kamarudin *et al.*[212] tested the breakdown performance of a mixture of CF_3I and CO_2 (30%:70% mixing ratio) under three kinds of electrodes (rod, plate, and coaxial electrodes) under a lightning impulse voltage. The tests were conducted, and it was assumed that CF_3I gas mixtures could be used in medium voltage (MV) equipment without involving arc extinguishing equipment. Youping *et al.*[213] tested the breakdown characteristics of the mixed gas of CF_3I and N_2 in a uniform electric field and concluded that the decomposition products of CF_3I would affect the insulation properties. The insulation performance of 30% CF_3I-70% N_2 at 0.1 MPa was similar to that of 20% SF_6-80% N_2 by DC voltage and lightning impulse voltage. Widger *et al.*[214] tested the insulation properties of a 30% CF_3I–CO_2 mixture in a ring-grid cabinet with a vacuum circuit breaker. It was demonstrated by laboratory tests that the gas mixture at this ratio met the requirements for medium-voltage equipment. Chen measured the 50% breakdown voltage of the 30/70% CF_3I/N_2 mixture at the lightning impulse voltage of a coaxial electrode. In order to explore the feasibility of the CF_3I–CO_2 mixture in a 400 kV gas-insulated power transmission line (GIL), the experiment was conducted under the equivalent similarity model with the same electric field distribution.[215] The possibility of the CF_3I/CO_2 mixture for insulation equipment was analyzed from the breakdown performance. It was considered that this gas was not suitable for the arc extinguishing medium, but it can be considered for use in the GIL.[216] The breakdown voltage of CF_3I mixed with CO_2 and N_2 showed a ternary mixed gas and no significant synergistic effect, and under the same conditions, the CF_3I and CO_2 mixed gas has better breakdown characteristics than CF_3I–N_2. This phenomenon was explained by measuring the decomposition products, and calculations showed that CO_2 could provide C atoms for the self-recovery of CF_3I molecules.[217]

de Urquijo[218] measured the electron swarm parameters of the CF_3I and N_2 mixed gas, including the ionization coefficient, attachment coefficient, drift velocity, and diffusion coefficient. The $(E/N)_{cr}$ of CF_3I was about 437Td, much larger than that of SF_6. The breakdown field of the 70%CF_3I–N_2 mixture is equal to that of SF_6. Kawaguchi *et al.*[219] calculated these parameters using the Monte Carlo algorithm and found good agreement with the experimental results. Kimura and Nakamura[220] calculated the electron swarm parameters of the mixed gas of CF_3I with CO_2. Li *et al.*[221] calculated the electronic swarm parameters of CF_3I mixed with a variety of gases such as CF_4, CO_2, N_2, O_2, and air. CF_3I mixed with N_2 and air has more significant advantages, and when the mixing ratio of CF_3I exceeded 70%, the breakdown field can exceed pure SF_6. Yun-Kun and Deng-Ming[222] and Deng and Xiao[223] have done a similar calculation. Combining the boiling point and the greenhouse effect, the feasibility of using CF_3I in high-pressure equipment was analyzed. It was considered that the mixed gas containing 70% CF_3I had the same dielectric strength as SF_6. Li[224] established the model to calculate the discharge process of CF_3I and calculated the time and process of the formation of the streamer current from the electron avalanche to the electron reaching the cathode.

Taki *et al.*[225] studied the interruption capability of CF_3I. First, the arc time constant and arc power loss coefficient were obtained by using Mayr's equation. The order of the arc time constant was SF_6, CF_3I, CO_2, H_2, Air, and N_2, while that of the arc loss coefficient was H_2, SF_6, CO_2, Air, N_2, and CF_3I; the short circuit fault interruption performance of CF_3I is tested, which can reach 90% of SF_6. When the volume ratio of CF_3I exceeded 20%, the interruption ability of CF_3I mixed with CO_2 approached pure CF_3I levels. The Breaker Terminal Failure (BTF) interruption capabilities of CF_3I and the mixed gas were tested. The BTF interruption capacity of CF_3I–CO_2 (30%–70%) was about 67% of SF_6.[226,227] Yokomizu *et al.*[228] calculated the electrical conductivity and thermal conductivity of CF_3I mixed with CO_2 at high temperatures and calculated transient parameters during quenching. When the temperature was above 10 000 K, the conductivity was greatly affected by the content of CF_3I. At 7000 K, the thermal conductivity was greatly affected by the content of CF_3I. The calculated results showed that the decay rate of the CF_3I mixed gas with CO_2 was weaker than that of SF_6, and the breakoff capacity was worse than SF_6 as a whole. Cressault *et al.*[229] calculated the plasma thermodynamic parameters (mass density, enthalpy, and specific heat) and transport parameters (viscosity, thermal conductance, and conductance) of CF_3I mixed with CO_2, N_2, and air. The calculated results showed that CF_3I mixed CO_2 is superior to the other two mixed gases because CO_2 plasma has better heat dissipation ability under a high temperature.

Ngoc *et al.*[230] tested the DC breakdown voltage of CF_3I and mixed N_2 at a quasi-uniform electric field (ball–ball electrode). The breakdown voltage of pure CF_3I was greater than that of SF_6, but the synergistic effect with N_2 was not obvious. With the increase in the CF_3I mixing ratio, the breakdown voltage also increased. When the mixing ratio of CF_3I was less than 50%, the breakdown voltage of the mixed gas was lower than the SF_6–N_2 mixed gas with the same ratio. After the breakdown experiment, it was found that solid iodine was deposited on the electrode surface. Kasuya *et al.*[231,232] tested the decomposition products of the CF_3I–CO_2 (30%–70%) mixed gas during quenching and improved iodine deposition by adding adsorbents. Continuous breakdown of CF_3I for 1300 cycles resulted in a 11% reduction in breakdown voltage.[233] The solid iodine also was generated by CF_3I–CO_2 gas mixture breakdown at the lightning impulse voltage.[234–236] Jamil *et al.*[237] quantitatively detected C_2F_6, C_2F_4, C_2F_5I, and a few C_3F_8, CHF_3, C_3F_6, and CH_3I within 224 h of CF_3I partial discharge under a non-uniform field. The presence of H_2O and O_2 would have an impact on the formation of decomposition products during discharge of CF_3I and accelerates the decomposition of CF_3I and produce toxic substances such as CF_2O.[238,239]

Although CF_3I has high insulation properties, it cannot be used alone in equipment due to the boiling point. Under the premise of ensuring the boiling point, the mixed gas with the buffer gas added cannot reach the level of pure SF_6, and there is no obvious arc extinguishing advantage. After the gas discharge, the obvious solid main atoms are generated (I and C), which is very detrimental to gas self-recovery in the use of the device. The oxidation of materials due to the presence of iodine could not be ignored. Its acute toxicity is acceptable, but this gas is genotoxic, so the safety of practitioners is a threat in the long-term operation of the device. Although a great deal of exploration has been done, all these achievements are carried out in the laboratory, and it is unlikely that the gas will be used in the equipment at present.

2. Mixtures of C_4F_7N with natural gases

In addition to the above gases, the bond in the carbon–fluorine bond is broken and replaced by atoms such as N to form some new

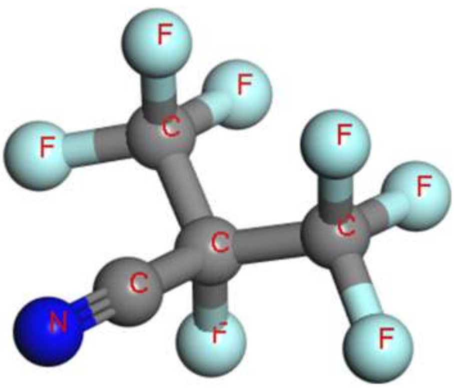

FIG. 10. Molecular structure of C_4F_7N.

derivatives such as C_4F_7N, the molecular structure of which is shown in Fig. 10.

In 2015, Alstom and 3M collaborated to test the power frequency dielectric strength of the C_4F_7N– CO_2 mixture in a 145 kV GIS. The study found that when the content of C_4F_7N is 18%–20%, it can achieve the same dielectric strength as pure SF_6.[47] The frequency and lightning impulse breakdown of the C_4F_7N/CO_2 mixed gas under different electric field types were tested under the influence of the mixing ratio, electrode distance, and gas pressure by Nechmi *et al.* from the French National Academy of Sciences AMPERE Lab.[240] It was found that the synergistic effect of C_4F_7N and CO_2 at a concentration of 3.7% was obvious. At present, the C_4F_7N/CO_2 mixed gas (g3) is tested in a 420 kV GIL and 245 kV current transformers. Owens[241] conducted the breakdown test of C_4F_7N with CO_2, N_2, and dry air mixtures at different pressures on a plate–plate electrode and found that the mixture had the best dielectric strength with CO_2. Preve *et al.*[242] tested the dielectric strength of the C_4F_7N/dry air mixture and found that its insulation properties were superior to SF_6 at impulse voltage but slightly inferior to SF_6 at AC voltage. Kieffel *et al.*[243] also conducted a continuous 100-s breaking test on C_4F_7N/CO_2 (the mixing ratio of C_4F_7N is 4%), with an average arcing time of 12 ms, which was lower than that of pure SF_6 (15 ms) at the same pressure.

C_4F_7N has a very high dielectric strength and is currently the most promising alternative to SF_6 in existing gases. However, the presence of a cyano-group (C≡N) in the molecule can be a hazard to the safety of the gas used in the equipment and the toxicity of the pure gas is not yet demonstrated, especially regarding neurotoxicity. Its main decomposition products and reaction with the molecules in the environment have also drawn attention.[244,245] For C_4F_7N, there may be some highly toxic by-products, such as CO and PFIB (C_4F_8), after 100 C–O 630 A/24 kV, the LC50 (4 h on mice) in an 11-l epoxy bulb of C_4F_7N/air or C_4F_7N/CO_2 mixture is inferior to 225 ppm.[246] Sulbaek Andersen *et al.*[247] measured the possible chemical reactions of C_4F_7N with OH, Cl, and O_3 in the atmosphere and found the products to be COF_2 and CF_3COF. The GWP of the gas was evaluated based on the infrared absorption spectrum. Due to the low content of the gas, the decomposition products did not adversely affect the environment. Blázquez *et al.*[248] calculated the reaction of gas molecules with OH radicals using the quantum chemical calculation method and obtained the reaction rate at 278–358 K.

The calculation of the molecular structure based on DFT mainly refers to the binding energy, ionization energy and molecular orbital gap, and decomposition process of the gas molecules.[249] The breakdown voltage of C_4F_7N/N_2 at power frequency voltage for 30 times does not change much, but a series of products are produced, such as CF_4, C_3F_8, CF_3CN, C_2F_4, C_2F_5CN, and C_3F_6.[250] It is noteworthy that the formed CF_3CN and C_2F_5CN are highly toxic gases and the toxicity of the gas C_4F_7N also needs further research and confirmation.[251] C_4F_7N would further react with H and OH, and the main production are CF_2HCN, CFH_2CN, CF_3CHFCN, and CF_3CH_2CN.[252] The computational decomposition process was studied, and the reaction of the molecules within the device with the metal Cu and Al surface was considered.[253,254]

The gas is currently a research hotspot and also has great potential for the gas medium used in high-voltage equipment. Due to the current use of less gas, the price of gas is relatively expensive. The gas greenhouse effect is low for high voltage applications and still high for medium voltage applications, while maintaining a low mixing ratio can still meet the equipment requirements of the insulation operation. However, due to the cyano group (C≡N) contained in the molecular structure, the free radical may react with others or atoms and even the metal in the device during discharge to generate toxic substances such as HCN and CuCN. This section needs further research and exploration to avoid the health threats.

3. Mixtures of perfluoroketones ($C_5F_{10}O$ and $C_6F_{12}O$) with natural gases

In 2015, ABB proposed to consider the use of ketones $C_5F_{10}O$ or $C_6F_{12}O$ (boiling points of 26.5 °C and 49 °C, respectively) in combination with the buffer gas as an insulating medium.[255] The molecular structures are shown in Fig. 11.

For the insulation properties, Mantilla *et al.*[255] found that the 50% positive lightning impulse breakdown voltage of a mixture of 5% $C_5F_{10}O$ and dry air at 0.7 MPa reached that of pure SF_6 at 0.4 MPa. Simka and Ranjan[256] tested the breakdown frequency field of $C_5F_{10}O$ and dry air under a quasi-uniform electric field and found that the critical breakdown strength of the mixed gas containing 5.2% $C_5F_{10}O$ at 0.7 MPa can reach 95% of pure SF_6 at 0.45MPa % and 80% of pure SF_6 at 0.6 MPa. For the engineering applications, Saxegaard *et al.*[257] found that the lightning impulse withstand level increased by 60% and the power frequency voltage level increased by 44%, by filling a 12 kV air switch cabinet with the $C_5F_{10}O$–air mixture. Hyrenbach and Zache[258] has produced a switchgear insulated with the $C_5F_{10}O$ mixed gas, which was commissioned in 2015 in a substation of Zurich. The switchboard passed the IEC62271-200 standard requirements of the full voltage test, and at this stage, $C_5F_{10}O$ mixed with air can be used for medium voltage equipment (6–40.5 kV). The switchboard with $C_5F_{10}O$ as the insulating medium is developed by ABB, and the gas chamber is made of stainless steel to prevent the metal materials inside the equipment from being oxidized.

By calculating the thermodynamic parameters and transport parameters of plasma at a high temperature of $C_5F_{10}O$ gas molecules,

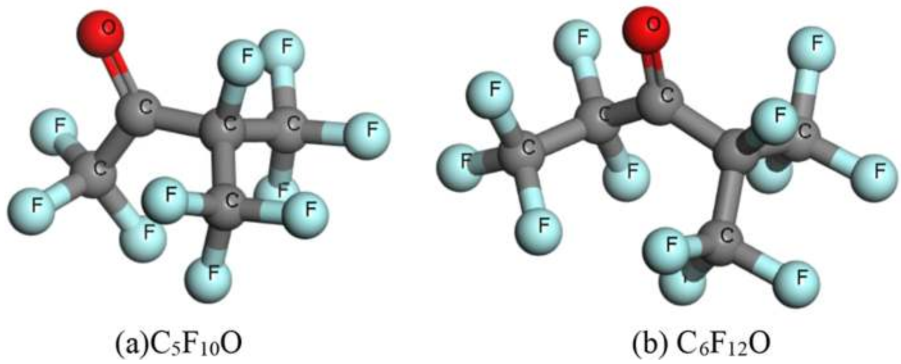

FIG. 11. $C_5F_{10}O$ and $C_6F_{12}O$.

it is considered that it has a better arc extinguishing property than SF_6 from the nature of transport. Part of the particle structure is complex, so its parameters (such as partition function and polarizability) have no reference data, which are calculated by computational chemistry.[259] However, Zhong *et al.*[260] calculated the thermodynamic properties of $C_5F_{10}O$ mixed with CO_2 and O_2. The calculation results showed that due to decomposition of $C_5F_{10}O$ in the process of quenching, the gas at the end of quenching cannot completely recover. The main products were CF_4, CO_2, C_4F_6, and graphite carbon. O_2 were added to the mixture without affecting the thermodynamic parameters and transport parameters. Therefore, the existing equipment is used in a mixture of $C_5F_{10}O$ and air.

Tatarinov *et al.* explored the decomposition products of $C_5F_{10}O$-dry air mixed gases under the application of 10 kV dielectric barrier discharge (DBD) and found that C_4F_{10}, C_6F_{14}, C_3F_6, C_5F_{12}, and other substances were produced.[261] Based on the optimization of the molecular model, the carbonyl carbon atom is the active site of C5-PFK molecules, and the decomposition of C5-PFK may take place centered on the carbonyl carbon atom.[262–264]

At the same time, the impact of C5 on the environment and personal safety also attracted attention. ABB tested the gas composition of the GIS with AIRPLUS gas ($C_5F_{10}O$ and air) during normal operation and gas leakage.[265] The mixture is not to be a threat to the environment or human body, but the LC50 (4 h) for mice after breaking tests lead to 2100 ppm, which is far lower than the one of gas mixture before breaking.[246]

For $C_6F_{12}O$, because of the high boiling point of the gas, the mixing ratio is seldom used in the equipment. Under the frequency test, adding 3% $C_6F_{12}O$ to N_2 can increase the breakdown voltage of pure N_2 almost by 1 time.[79] The products after breakdown are PFCs and thus have no effect on the insulation properties. The content is low, which will not affect the environment. It is considered that the gas is more suitable for use in medium and low voltage equipment. By adding a small amount of $C_6F_{12}O$ in N_2, the insulation level of the equipment is improved. Existing studies have shown that the $C_6F_{12}O/CO_2$ mixed gas has the potential for application in a 10 kV switchgear.[266,267]

The gas insulation far exceeds SF_6, but the problem of boiling point has also become very prominent. At present, $C_5F_{10}O$ is expected to be the main insulating gas for medium voltage equipment.

The main properties of C_nF_mX mixtures are shown in Table VIII of the Appendix.

E. Others

Since C atoms and F atoms have good electronegativity, the gas molecules, formed by the combination of C and F with other atoms such as H, Cl, S, and N, generally also have good insulation properties. Devins in 1980 summarized the basic insulation properties of gases,[32] such as CF_nCl_{3-n}, CHF_nCl_{3-n}, and C_nH_{2n+2}; their insulation properties gradually increased with the increase in n, but the boiling point was also gradually obvious. However, some gases have the greenhouse effect, and some were toxic gases such as CF_3CN. Therefore, there was not much gas available for reference at the moment.

CF_3NSF_2 was also considered to have high-performance gas insulation, the insulation performance of about 2.41 times the SF_6, and the boiling point of $-6\,^{\circ}C$. Cheng *et al.* calculated the reaction mechanism of this molecule with OH.[268] The literature for the study of this gas is still relatively less, and the field of its application is relatively vague now. The gas products available are difficult to supply. There is not much literature on the experimental research of its various properties.

CCl_2F_2 (R12) is a Freon gas with a GWP of 2400 that is far less than that of SF_6. The experimental study found that the insulation strength of the gas was about 90% of that of SF_6. The mixed gas showed good self-stability through mixed air and N_2 breakdown experiments.[48] However, this gas has a large damage to the ozone layer, with the ozone depletion potential (ODP) up to 1.0.

HFO1234zeE ($CF_3CH{=}CHF$) is non-toxic, non-flammable, and non-destructive of the ozone layer, with a GWP value of less than 0.02 and the lifetime of 1 day. It is generally used as a refrigerant. Through the application of AC and positive and negative lightning impulse voltage, the breakdown test was studied under the uniform field and extreme non-uniform field. HFO1234zeE showed very similar insulating properties to SF_6. It can therefore be considered as a substitute for medium-voltage equipment.[49] For the electron swarm parameter of the HFO1234zeE molecule under PT discharge, the gas was found to have strong electron attachment capacity.[269] In medium- or high-voltage applications, the HFO1234zeE/N_2 mixture would show more excellent electrical strength in the range of 100 kPa to 1 MPa than currently obtained at 10 kPa. HFO1234zeE has comparable electrical strength to SF_6 at 130 kPa. There is no synergistic effect in the HFO1234zeE/N_2 and HFO1234zeE/CO_2 mixtures.[270] The main characteristics of this gas demonstrates that it can be used as a dielectric medium for the MV switchgear, but it cannot be used in breaking.[271]

Chen[272] analyzed the molecular structure of OCCHCN and concluded that it was not easily ionized and excited based on quantum chemistry calculation, but there was no experimental data to validate it.

The insulation properties of gases can be predicted to filter potential alternative gases based on the calculation results. The parameters that affect the gas insulation performance are the relative molecular mass M, the dipole moment μ, the polarizability α, and so on. The ionization collisions increase the number of carriers, thereby weakening the gas dielectric strength. The electron attachment collision does not increase the number of carriers but can slow down carriers, which is helpful to strengthen the dielectric strength. Molecules with higher ionization energy are more susceptible to ionization collisions. More electronegative molecules attach electrons more easily, so insulating gas should have higher ionization energy (IE) and electronegativity.

Yu[58] builds the new structure-activity relationship (SAR) models to calculate the molecular insulation properties by combining the surface area, polarizability, electronegativity, and molecular hardness of a molecule or functional group. Through the calculation of the existing molecules, it is found that the functional group CF_3 has outstanding dielectric strength in the molecular structure due to its large surface area and polarizability. At the same time, taking into account the impact of the boiling point, the authors believe that SF_5CN and SF_5CFO have greater potential to replace SF_6.

V. CONCLUSION AND OUTLOOK

A. Conclusion

Table IV shows the main alternative gases and their properties. The main studies of several major alternative gases now draw the following conclusions:

(1) For natural gas, the insulation performance is only 40% of SF_6 or even lower, but safety and low cost become the advantages. By optimizing the structure of the equipment, increasing pressure, and combining solid insulation, the natural gas could be used in medium and low voltage equipment.

(2) The research results of SF_6 mixtures are quite mature. SF_6/N_2 is a relatively stable combination for the moment and has been used in GILs and switchgear cabinets. However, studies have shown that CO_2 shows obvious thermodynamic properties at high temperatures despite the slightly lower insulating properties of CO_2 mixtures, and the sensitivity of the mixed gas to the electric field uniformity is lower than that of the N_2 mixed gas. For interrupter properties, the SF_6-CF_4 mixed gas has also been used in circuit breakers. As for decomposition performance, the decomposition products of the mixed gas are more complicated than pure SF_6. However, the reduced use of SF_6 also inhibits the production of toxic sulfur compounds.

(3) PFCs have some advantages over SF_6 in terms of GWP, and both theoretical calculations and experimental measurements show that the insulating properties of pure gas are superior to that of SF_6. Affected by the boiling point, the insulating properties of the mixture cannot reach the level of SF_6.

(4) Despite its superior gas-insulating properties and no greenhouse effect, the decomposition of CF_3I after discharge is the

TABLE IV. Basic properties of main alternative gases. G presents that the property is better than that of SF_6. NG presents that the property is worse than that of SF_6. E presents that the property is comparable to that of SF_6. – presents that the gases were studied but have no real application.

Gases	Boiling point	GWP/ODP	Insulation	Interruption	Decomposition	Application
SF_6	Good	Not good	Very good	Very good	Not good (toxic but in low concentration)	GIS/GIL/GCB/GIT
N_2	G	G	NG	NG	...	C-GIS(72 kV)
Air	G	G	NG	NG	...	C-GIS(40 kV)
CO_2	G	G	NG	NG	...	40 kV C-GIS 70 kV GCB
$SF_6 + N_2$	G	G	E	NG	G	245–550 kVGIL
$SF_6 + CO_2$	G	G	E	NG	G	...
$SF_6 + CF_4$	G	G	E	E	G	550 kV GCB
c-C_4F_8 mixtures	NG	G	E	NG	NG	...
C_3F_8 mixtures	NG	G	E	NG	...	...
C_2F_6 mixtures	NG	G	NG	NG	...	...
CF_4	NG	G	NG	NG	...	...
CF_3I mixtures	NG	G	E	NG	NG	...
$C_4F_7N + CO_2$	NG	G	E	E	NG in MV equipment than SF_6	420 kV GIL/245 kV CT
$C_5F_{10}O$ + air	NG	G	E	E	NG in MV equipment than SF_6	MV GIS(6–40.5 kV)
$C_6F_{12}O$ mixtures	NG	G	E	...	G	C-GIS(12 kV)
HFO1234zeE	G	G	E	NG	G	C-GIS (24 kV)

TABLE V. Basic properties of natural gases and mixtures.

Gases	Breakdown voltage/partial discharge voltages	Voltage/electrode	P (MPa)	Reference
N_2	The breakdown voltage can be increased by 1.5 times at 0.2 MPa by composite solid insulation.	AC/rod-plane	0.1–0.6	82
	The breakdown voltage is lower for positive polarity waveforms in the presence of a bias voltage.	Non-standard-LI rod-plane	0.7	87
	The breakdown voltage of N_2 at 1.0 MPa can be equal to that of 0.5 MPa SF_6.	LI/spherical-plane	0.6–2.0	94
CO_2	The breakdown values of CO_2 are more stable than those of N_2.	AC and LI plane-plane	0.7–1.1	84
	The breakdown voltage is lower for positive polarity waveforms in the presence of a bias voltage.	Non-standard-LI/ rod-plane	0.7	86
Air	The dielectric strength of air is higher than that of N_2 and CO_2 at 0.5 MPa based on the initial flashover voltage and the 50% flashover voltage.	LI/coaxial-cylindrical and parallel plate	0.1–0.5	91
	The partial discharge voltages of air and N_2 are almost the same, but the breakdown voltage of air is larger than that of pure N_2.	LI/rod-plane	0.1–0.4	93
N_2O/N_2	The dielectric strength for 20/80%N_2O/N_2 at 0.6 MPa showed a synergy effect.	DC/needle–plane	0.1–1.0	88
N_2–He	The breakdown voltage of N_2–He rises rapidly and then follows a linear behavior with the mixing ratio of N_2.	AC/plate-plate	<0.6	89
N_2/CO_2	The breakdown voltage of the 50%N_2/50%CO_2 mixture is only one-third that of SF_6.	LI/sphere-plane	01–30	83

Gases	Electron swarm parameters	Method	E/N (Td) T (K)	P (MPa)	Reference
Mixtures	Small additions of CO_2 (5%) produced a significant attachment in the air-CO_2 mixtures.	Measure	90–260 ...	10–100 Torr	100
	In the mixtures of CO_2 with both 50% O_2 and 50% H_2, $(E/N)_{cr}$ clearly shows higher values than in pure CO_2.	Calculation	0–200 300–3500	0.1 MPa	96
	Adding a small amount of O_2 to CO_2 can effectively improve the value of $(E/N)_{cr}$ with a clear synergistic effect.	Calculation	0–200 ...	0.1 MPa	97
	The reduced critical breakdown field of CO_2 with O_2 and CH_4 show higher values.	Calculation	0–150 300–4000	0.1 MPa	98
	The values of $(\alpha - \eta)/N$ for CO_2–N_2 mixtures are about 30 times smaller than those for CO_2–O_2 mixtures.	Measure/ calculation	0.01–1000 293–298	0.6–600 Torr	99

Gases	Interruption ability	Method	P (MPa)	Reference
Air/CO_2	For a fixed pressure, the gases were ranked in terms of arc interruption performance as follows, in increasing order: air, CO_2, and SF_6.	Measure/calculation 300–4000 K	0.5	103
Air	A low nozzle-to-contact diameter ratio is favorable in terms of requiring less upstream overpressure for successful interruption of air.	Measure/calculation Load currents: 300–900 A	0.05–1.4 bar (upstream)	107
CO_2	The thermal interruption capability of CO_2 could be estimated to be about 50% of that of SF_6.	Measure 84 kV GCB	...	108

TABLE VI. Basic properties of SF_6 mixtures.

Gases	Breakdown voltage/partial discharge voltages	Voltage/electrode	P (MPa)	Reference
$SF_6 + N_2$	SF_6–N_2 mixtures containing 50%–60% of SF_6 have a dielectric strength of up to 85%–90% that of pure SF_6.	AC/DC/LI Plate-plate/rod-sphere	0.1–0.5	113
	A simplified streamer criterion proposed for SF_6 can be used to calculate the discharge inception levels in SF_6–N_2 mixtures.	DC Sphere-plane/ sphere-sphere	0.1–0.5	114
	The addition of 0.1% of SF_6 into N_2 results in an increase in the breakdown voltage at pressures below 2.5 bars.	PI Rod-plane	0.1–0.5	115
	The dielectric strength of the 50% SF_6/N_2 mixture is about 8–12% higher than that of the 20% SF_6 gas mixture.	LI and AC Sphere-plane/rod-plane	0.3–0.7	118
	The increase in corona onset voltages with the increase in the amounts of SF_6. The values of positive polarity are higher to those obtained with negative polarity.	DC Tip-plane	0.3–1.5	119
	An increase in the GIS tank diameter of about 15% with the 10% SF_6–N_2 mixture at 0.6 MPa compared to pure SF6 at 0.4 MPa.	LI/SI/AC Coaxial cylinder	0.2–0.6	120
	N_2–SF_6 mixtures with a SF_6 content of 1%–20% and pressure of 0.71 MPa–1.24 MPa are more sensitive to fixed protrusions than pure SF_6 at 0.5 MPa of the same dielectric strength.	AC/LI/SI Needle-plane	0.5–1.24	144
	The negative synergistic effect of the SF_6/N_2 mixture appeared with low gas pressure.	LI Rod-plane	0.2–0.5	122
$SF_6 + CO_2$	With a single large protrusion on the electrode, the breakdown strength of the 50%SF_6–CO_2 mixture is slightly higher than that of SF_6.	AC Cylindrical	0.1–0.4	132
	With adding CO_2 to the N_2/SF_6 gas mixture, the breakdown values rise significantly, particularly at high pressures.	AC/LI Needle-plane	0.1–0.6	133
SF_6 + Air	The rate of rise impulse wave voltage has a significant effect on the breakdown voltage of 1% SF_6/air mixture.	LI/SI Coaxial cylinder/rod-sphere	0.1–0.5	129
	SF_6-air mixtures have corona stabilization and is higher than the corresponding values for SF_6–CO_2 and SF_6–N_2 mixtures.	DC Rod-plane	0.1–0.5	128
$SF_6 + CF_4$	The PD inception voltages have hardly any effect on mixed rate of SF_6 in 25.8 kV GIS	AC/LI Sphere-sphere	0.05–0.3	138
	SF_6-CF_4 mixtures under uniform fields have breakdown voltages that vary linearly with the SF_6 content. Under highly non-uniform fields, a corona stabilization may occur under positive impulse, positive DC and AC voltages leading to high breakdowns for the mixtures 10% SF6-90% CF4 to 25%SF_6–75%CF_4.	AC/LI/DC Sphere-sphere	0.2–0.4	140
	The AC corona inception occurred at lower voltage levels than DC. The average time to breakdown corresponding to negative lighting impulse breakdown voltages are generally shorter than those of positive	AC/DC/LI Sphere-sphere	0.3–1.0	142
$SF_6 + H_2$	The addition of 0.002% SF_6 to H_2 resulted in a substantial increase in AC breakdown voltage of typically 70%.	AC Rod-plane/ rod-rod	0.1–0.4	135
	The increase in negative breakdown voltage with the addition of small quantities (<1%) of SF_6 is smaller than for positive-impulse conditions	LI Rod-plane	0.05–0.3	136

TABLE VI. (*Continued.*)

Gases	Electron swarm parameters	Method	E/N (Td) T (k)	P (MPa)	Reference
$SF_6 + N_2$ $SF_6 + N_2O$	The breakdown is governed by the mean energy of SF_6 for low concentrations of SF_6 up to 10%, and only for still lower concentrations, the mean energy of electrons corresponds to that of N_2.	Calculation	700 273	. . .	148
$SF_6 + N_2$	The variation of the effective ionization coefficient is non-linear with the mixture ratio.	Measure SST	182–258 293	0–100 Torr	150
$SF_6 + N_2$	The variation of the effective ionization coefficient does not vary linearly with the ratio of the two gases in the SF_6–N_2 mixture. With an increasing SF_6 content in the mixture, a reduction in the apparent secondary ionization coefficient is observed.	Calculation	100–450 V cm^{-1} $Torr^{-1}$	5–40 Torr	151
$SF_6 + CO_2$	The rate of increase in the attachment coefficient with an increase in the percentage of SF_6 in the SF_6–CO_2 mixtures was much larger than the rate of change in the first ionization coefficient.	Measure (SST) sphere-sphere/ rod-rod	. . .	0.4	152
	CO_2 in SF_6–CO_2 mixtures can change the transport properties, but the effect of detachment is relatively slight on the properties of electrical discharge.	Calculation (PT) parallel plate	270–370	. . .	155
	The influence of SF_6 in the SF_6–CO_2 mixture is strongly apparent in the values for the effective ionization coefficients. The value of critical field strength E/N_{cr} is smaller than that measured for the SF_6–N_2 mixtures.	Measure (PT)	100–700 293–302	0–0.001	156
	At temperatures above 1750 K, an addition of CO_2 to SF_6 gas can enhance dielectric breakdown performances, while at low temperatures, too much CO2 added into mixtures can reduce dielectric breakdown abilities.	Calculation	. . . 300–3500	0.01–1.0	162
$SF_6 + CF_4$	After addition CF_4 to SF_6, the electron drift velocity in SF_6 and CF_4 increases, effective ionization coefficient decreases with the increase in the SF_6 content, and diffusion of CF_4 is stronger than that of SF_6.	Calculation (Monte Carlo)	150–500 293 K	1 Torr	158
	For higher gas temperatures (i.e., T > 2200 K at 0.4 MPa), the (E/N)cr in SF_6–CF_4 mixtures are obviously higher than that in pure SF_6.	Calculation (Boltzmann)	. . . 300–3000	0.01–1.6	162
	The mixture of SF_6 and CF_4 exhibits a suppressed CF_4 ionization and an increased SF_6 ionization in the mixture relative to pure CF_4 and SF_6.	Calculation	140–600 293 K	1 Torr	159
SF_6 + He	The addition of He to the gaseous mixture decreases the reduced critical electric field.	Calculation (Boltzmann)	. . . 300–3500	0.1–1.6	171
Gases	**Interruption ability**	**Method**		**P (MPa)**	**Reference**
$SF_6 + N_2$	Under two-temperature assumption, the electron conductivity of the SF_6–N_2 mixture is distinctly lower than that of pure N_2.	Calculation LTE/NLTE 300–40 000 K		0.1	173
	Mixing CO_2 with SF_6 at a certain ratio, compared to the case of pure CO_2, the largely preserved thermal cooling effect of SF_6 can favor the thermal recovery of circuit breakers during current interruption.	Calculation in LTE 300–30 000 K		0.01 and 1.6	170

TABLE VI. (*Continued.*)

Gases	Interruption ability	Method	P (MPa)	Reference
	The arc interruption capabilities of the SF_6–CO_2 mixture increase greatly with an increase in SF_6 concentration and are about 40%, 45%, and 70% that of SF_6 at a SF_6 content of 0%, 20%, and 50% in the applied puffer GCB test prototype and at a short-circuit current of 10 kA.	Measure short-circuit current: 10 kA	...	174
$SF_6 + CF_4$	The net radiation of a SF_6-CF_4 or SF_6–C_2F_6 mixture is always greater than that of pure SF_6. The SF_6/CF_4 mixture has interruption properties very close to those of pure SF_6 as long as the proportion of SF6 is about 50%.	Calculation in LTE 300–30 000 K	0.1	168,169
	An SF_6/CF_4 filled circuit breaker often retains its breaking capacity down to the lowest ambient temperatures.	Measure TFT/SFT	0.5,0.7	172
SF_6 + Ar	The diameter of the Ar/SF_6 (20%) arc was smaller than that of the Ar arc. Before interrupting the arc current, the electron density of the Ar/SF_6 (20%) arc was larger than that of Ar. After the current interruption, however, the electron density of the Ar/SF_6 (20%) arc decreased rapidly.	Measure (LTS)	0.1	166
Gases	**Decomposition products**	**Method**	**P (MPa)**	**Reference**
$SF_6 + CF_4$	The gaseous by-products of the spark decomposition of mixtures included $SOF_2 + SF_4$, SOF_4, SO_2F_2, S_2F_{10}, S_2OF_{10}, $S_2O_2F_{10}$, and $S_2O_3F_6$ with O_2 and H_2O.	AC sparks discharge Point-insulator-plane	0.1	176
$SF_6 + N_2$	The decomposition products SOF_4, SO_2F_2, $SF_4 + SOF_2$, SO_2, S_2OF_{10}, S_2F_{10}, $S_2O_2F_{10}$, $S_2O_3F_6$, SF_5NF_2, NF_3, and $(SF_5)_2NF$ were assayed.	DC/AC corona discharges Point-plane	0.4	179
$SF_6 + O_2$	The yields of SOF_4, SO_2F_2, SOF_2, and SO_2 have been measured as a function of O_2 content in SF_6/O_2 mixtures.	Spark discharges Cylindrical	0.133	178
$SF_6 + CO_2$	The presence of CO_2 in SF_6 and SF_6–N_2 mixtures leads to a considerable increase in the formation of ($SOF_4 + SO_2F_2$) and decreased formation of S_2F_{10}.	Corona discharges Point-plane	0.4	182

biggest drawback, which also limits its use in equipment. The solid iodine and carbon deposited on the surface of electrodes, which is detrimental to the gas self-healing, so the gas is not suitable for use in the interrupter medium. Its genotoxicity is also a major obstacle.

(5) C_3F_7N has a great insulating property so that the mixed gas (at a very low mixing ratio) can still reach the insulation level of SF_6 for high voltage equipment. Mixed gases are currently used in GIS and circuit breakers. It is noteworthy that the decomposition of gas discharge may produce some of the toxic gases or solid products, which requires further study and verification.

(6) Perfluoroketones, mainly $C_5F_{10}O$, have similar insulation properties of C_4F_7N. However, using mixed gas is more suitable for medium voltage equipment due to the higher boiling point than C_4F_7N and the too high value of GWP of C_4F_7N. Air is used in the mixture to prevent oxidation inside the equipment. The decomposition product after discharge will not affect the environment and the human body.

(7) For other gases such as HFO1234zeE, some research studies have not reached a mature conclusion, so their potential for substitution remains to be further studied.

B. Outlook

Through the above research on the current alternative gases, the research on alternative gases mainly focuses on the insulation performance, the arc-extinguishing performance, and the decomposition characteristics.

(1) For insulation properties, the experimental parameters measured are relatively easy to obtain. The gas insulation can be evaluated by comparing with the SF_6. Setting different electrodes, voltage type, pressure, and mixing ratio has become common experimental means to comprehensively investigate the insulation properties of gas. The inception voltage

TABLE VII. Main properties of PFCs and mixtures.

Gases	Breakdown voltage/partial discharge voltage comment	Voltage/electrode	P (MPa)	Reference
c-C_4F_8/1-C_3F_6/ C_3F_8/C_2F_6 + N_2/ CO_2/CF_4	Positive synergism was observed for gas mixtures with a PFC gas (c-C_4F_8, 1-C_3F_6, C_3F_8 and C_2F_6) and any of N_2, CO_2, and CF_4 gases.	AC Rod-plane	0.10–0.40	180
c-C_4F_8/N_2	The sparkover voltage of c-C_4F_8 is about 1.3 times and 1.3–1.4 times higher than SF_6.	AC/LI Parallel-plane	0.1	186
c-C_4F_8/N_2	The breakdown voltage of the c-C_4F_8/N_2 mixture under negative lighting impulse is lower than that under positive polarity. c-C_4F_8/N_2 mixtures show the synergistic effect.	LI Sphere-plane	0.1–0.3	188
C_3F_8/N_2 C_2F_6/N_2	In C_3F_8/N_2 and C_2F_6/N_2 mixtures, the synergistic effect in electrical insulation performance was less remarkable than that in SF_6/N_2 mixtures.	AC Needle-plane	0.1	190
C_3F_8+ air	Both breakdown ratios of C_3F_8 to air approach a minimum of about 2.5 at the sphere–plane electrode system.	LI Sphere-plane/ point-plane	0.1	189
CF_4	CF_4 has a smaller critical field strength and is less attaching than SF_6.	AC/DC/LI Point-plane	0.1–0.4	199
	At large values, pL > 2 Torr cm, the rate of growth of breakdown voltage with pressure essentially increases due to the attachment.	DC Plane-plane	0.1–10 Torr	202

Gases	Electron swarm parameters	Method	E/N (Td) T (K)	P (MPa)	Reference
c-C_4F_8	A critical field strength E/Ncr of c-C_4F_8 is 439.5 td.	Measure (PT) 12 Td-43 Td	330–600 292–300 K	1–7.5Torr	191
c-C_4F_8 + SF_6	The limiting E/N of 20% SF_6 and 80% c-C_4F_8 can exceed the values for the respective pure gases.	Calculation	282–707 273 K	1 Torr	192
c-C_4F_8 + CO_2	The limiting field $(E/N)_{lim}$ of the c-C_4F_8/CO_2 mixtures is higher than that of SF_6/CO_2 mixtures.	Calculation (Monte Carlo)	150–450 293 K	1 Torr	194
c-C_4F_8 + N_2 c-C_4F_8 + air	c-C_4F_8–N_2 and c-C_4F_8–air have very similar (E/N)cr values, higher than those of the other three mixtures (CO_2, CF_4, and O_2), and superior even to that of pure SF_6 for c-C_4F_8 concentrations above 80%.	Calculation	150–600 300 K	0.1	195
C_3F_8 + N_2	The limiting field strength of the C_3F_8–N_2 gas mixture is greater than that of C_3F_8–CO_2.	Calculation	1–1000 293	1 Torr	196
CF_4	Replacing SF_6 with CF_4 brings an increase in the critical reduced electric field strength for temperatures above 2200 K.	Calculation	0–1000 T 300–35 0	0.01–1.6	201
C_3F_8 + N_2	The C_3F_8–N_2 mixture has the largest (E/N)cr of the cold C_3F_8-CF_4, C_3F_8–CO_2, C_3F_8–N_2, C_3F_8–O_2, and C_3F_8–Ar. The hot C_3F_8 gas gas has much poorer dielectric performance than hot SF6 because the (E/N)cr of C3F8 decreases significantly above room temperature.	Calculation	100–600 300–3 500	0.01–1.6	200

Gases	Decomposition	Method	P (MPa)	Reference
c-C_4F_8 c-C_4F_8 + N_2	The main identified gaseous by-products are CF_4, C_2F_6, C_2F_4, C_3F_8, and C_3F_6 for pure c-C_4F_8 gas and CF_4, C_2F_6, C_2F_4, C_3F_8, C_3F_6, and C_2F_3N for the c-C_4F_8/N_2 mixture.	50 Hz ac corona discharge Needle-plane	0.1	205

TABLE VIII. Main properties of C_nF_mX mixtures. DBD-Dielectric Barrier Discharge. 1 Torr = 133.3Pa.

Gases	Breakdown voltage/partial discharge voltages	Voltage/electrode	P (MPa)	Reference
CF_3I/N_2	The optimum ratio of CF_3I/N_2 to replace SF_6 gas as an insulating medium is 30% at 0.3 MPa based on the breakdown characteristics.	AC Needle-plate	0.1–0.3	208
	Under 0.1 MPa and 0.2 MPa, 30%CF_3I/70%N_2 present similar insulation properties as 20%SF_6/80%N_2.	DC/LI Plane-plane	0.1 and 0.2	213
	Based on the 50% breakdown voltage of the CF_3I/N_2 gas mixture. The CF_3I mixture has the potential to replace SF_6 as an insulation medium in GIL.	LI Coaxial cylindrical	0.1–0.3	215
	The breakdown voltage of CF_3I–N_2 mixtures increases proportionally to the CF_3I content without the synergistic effect. The breakdown voltages for mixtures of 50% CF_3I are lower than with SF_6 at the same ratio.	DC Sphere-sphere	0.1–0.6	230
CF_3I/CO_2	When the RMU vacuum circuit breakers are insulated with a 30%:70% CF_3I–CO_2 mixture, no disruptive discharges are detected for a 50 impulse test series.	LI RMU	0.14	214
	The 50% breakdown strength of the 30:70% mixture of CF_3I–CO_2 for the coaxial electrode was more than two times higher than air.	LI Rod-plane/ plane-plane/ coaxial cylindrical	0.1	212
	The PDIV+ of CF_3I/CO_2 is higher than that of SF_6/CO_2 when k is10%–40%. The PDIV+ of CF_3I/CO_2 (30%–40%) at 0.15–0.2 MPa can reach the level of pure SF_6 at 0.1 MPa.	AC Needle-plate	0.1–0.3	209
CF_3I–air	Pure CF_3I gas has 1.2 times as high a dielectric strength as pure SF_6 gas at the same pressure. V–t characteristics in CF_3I–air gas mixtures are almost the same as those in CF_3I–N_2 gas mixtures.	Steep-front square voltage Rod-plane	0.1	210
$C_4F_7N + CO_2$	The content of C_4F_7N was 18%–20%, and it can achieve the same dielectric strength as pure SF_6.	AC inhomogeneous field	0.15, 0.19	47
$C_4F_7N + CO_2$	The synergistic effect of C_4F_7N and CO_2 at a concentration of 3.7% is obvious, and the mixture in uniform electric field reaches 72% of of the dielectric breakdown of pure SF_6 at 0.55 MPa.	AC/LI plane-plane/ sphere-plane/rod-plane/ sphere-sphere	0.1–1.04	240
C_4F_7N + CO_2/n_2/air	The dielectric breakdown strength of the gas mixture increases at higher pressures and increased C_4F_7N concentration.	Disk electrodes	0.1–1.1	241
$C_5F_{10}O$ + air	The air PFK-max mixture at 0.7 MPa has about 95% the withstand capability of 0.45 MPa SF_6.	Step-DC Sphere-sphere	0.1–0.7	250
$C_5F_{10}O$ + air $C_6F_{12}O$ + air	The breakdown performance of the investigated mixtures can approach SF_6 values at increased total filling pressures.	AC/LI Sphere-sphere	0.1–0.7	249

Gases	Electron swarm parameters	Method	E/N (Td) T (K)	P (MPa)	Reference
$CF_3I + N_2$	The limiting field strength of CF_3I was found to be E/Nlim = 437 td. For the CF_3I–N_2 mixture with 70% CF_3I, this E/Nlim value was found to be essentially the same as that for pure SF_6.	Measure PT	100–850 293–301	0.4–20 Torr	218
$CF_3I + CF_4$/ N_2/CO_2/ O_2/air	The (E/N)cr of CF_3I–N_2 and CF_3I–air are obviously higher than that of SF_6–N_2 at the CF_3I ratio higher than 65% and even higher than 65% and even higher than that of pure SF_6 at the CF_3I ratio ratio higher than 70%.	Calculation	0–600 300	. . .	221
$CF_3I + N_2$/ CO_2	For the mixtures with 70% CF_3I, the values of (E/N)lim are essentially the same as that for pure SF_6.	Calculation SST	100–1000 293	1 Torr	222

TABLE VIII. (*Continued.*)

	Breakdown voltage/partial discharge voltages	Voltage/electrode			
Gases	Electron swarm parameters	Method	E/N (Td) T (K)	P (MPa)	Reference
CF_3I + Ar/Xe/He/N_2/CO_2	Among the mixtures of CF_3I with Ar, Xe, He, N_2, and CO_2, $CF_3I–N_2$ present the greatest insulation strength with 20%–90% CF_3I content based on (E/N)cr.	Calculation SST	100–800 293	1 Torr	223
Gases	Interruption ability	Method		P (MPa)	Reference
$CF_3I + CO_2$	The interruption performance of the CF_3I/CO_2 mixture approximated that of pure CF_3I when the ratio of CF_3I exceeds 20%.	Measure/SLF frequency of oscillating current: 45 kHz.		0.2 (upstream)	218
	In BTF interruption, $CF_3I–CO_2$ is superior to $CF_3I–N_2$ and the performance approximates to that of pure CF3I when the proportion of CF3I exceeds 30%.	Measure/BTF Peak of current: 3.0 kA.		0.2	225
	The arc conductance attenuated more rapidly for CO_2 mixed with CF_3I at concentrations above 0.9 than for pure CO_2.	Calculation in LTE 300–30 000 K		0.1,0.5	228
$CF_3I + CO_2$/N_2/air	CF_3I has a rather small low-temperature electrical conductivity (lower than SF_6).	Calculation LTE 300–50 000 K		0.1–3.2	229
$C_4F_7N + CO_2$	The arcing time is stable over the 100 operations, and the average arcing time is about 12 ms compared to a typical value of 15 ms for SF_6.	Measure 420 kV disconnector		0.55	243
$C_5F_{10}O$ + air	The pressure peak is up to 30% higher compared to SF_6 and the peak for SF_6 is reached in 17 ms, while for the mixture, it is reached in 10–12 ms.	Measure GIS short circuit current: 40 kA		...	253
$C_5F_{10}O$	The arc interruption performance and electric strength of C5-PFK are comparable to or better than those of SF_6.	Calculation 300–30 000 K		0.1–1.0	254
Gases	Decomposition characteristics	Method		P (MPa)	
CF_3I	The partial discharge by-products of C_2F_6, C_2F_4, C_2F_5I, C_3F_8, CHF_3, C_3F_6, and CH_3I were obtained.	Experiment AC/needle-plane		0.1	237
$CF_3I–CO_2$	CF_3I gas generates iodine after current interruption.	Experiment SLF and BTF		0.2	231
	Iodine is deposited on the electrode along with carbon and oxygen after $CF_3I–CO_2$ gas mixtures discharge under a positive impulse polarity.	Experiment LI/rod-plane		0.1–0.2	234
$CF_3I + H_2O$	The decomposition products of CF_3I include the main components C_2F_6, I_2 and other components such as C_2F_4, C_2F_5I, C_3F_8, HF, H_2, COF_2, CF_3H, and CF_3OH with a small amount of H_2O.	Calculation		...	238
$CF_3I + O_2$	The breakdown decomposition rate of CF_3I is accelerated, and COF_2 is produced in the presence of O_2.	Measure and Calculation/AC		...	239
C_4F_7N + air $C_4F_7N + CO_2$	CO and C_4F_8 are produced after the breaking test, and the LC50 (4 h on mice) after 100 C–O 630 A/24 kV in an 11-l epoxy bulb is inferior to 225 ppm.	Measure 100 C–O 630 A/24 kV		0.174	246
C_4F_7N + air	The sole atmospheric degradation products appear to be NO, COF_2, and $CF_3C(O)F$.	Measure and calculation/296 ± 1 K		700 Torr	247

TABLE VIII. (*Continued.*)

Gases	Breakdown voltage/partial discharge voltages Interruption ability	Voltage/electrode Method	P (MPa)	Reference
$C_4F_7N + CO_2$	The decomposition rate of C_3F_7CN and generation rate of the products increase with the increase in ambient temperature.	Calculation (2 000–3 000 K)	0.1	249
C_4F_7N + Cu/Al	The adsorption energy of C_3F_7CN adsorbed on Cu (1 1 1) and Al (1 1 1) is both below 0.8 eV.	Calculation	. . .-	253
$C_5F_{10}O$ + Air/ N_2/CO_2	After the DBD processing of two test-gases, a large quantity of of toxic C_3F_6 was found in pure $C_5F_{10}O$.	Measure DBD	0.1	258
$C_5F_{10}O$ + Air	CO and C_4F_8 are produced after the breaking test, and the LC50 (4 h on mice) after 100 C–O 630 630 A/24 kV in an 11-l epoxy bulb is inferior to 2100 ppm.	Measure 100 C–O 630 A/24 kV	0.125	246
$C_5F_{10}O + N_2$	The amount of decomposition products of $C_5F_{10}O$ (CF_4, C_2F_6, C_3F_6, C_3F_8, C_4F_{10}, and C_6F_{14}), increased with the increased number of discharges.	Measure calculation AC/sphere-sphere	0.11	262
$C_6F_{12}O + N_2$	The breakdown decomposition products of $C_6F_{12}O + N_2$ were CF_4, C_2F_6, C_3F_6, C_3F_8, C_4F_{10}, and C_5F_{12}.	Measure calculation AC/sphere-sphere	0.1	79

measurement for partial discharge is already there. The calculation of the discharge process of PD or discharge by Townsend discharge theory has also been verified.

The measurement process is generally at a low pressure (1 Torr), and there is a deviation of the calculation results of the gas insulation performance under high pressure. The calculated value is derived from the collision cross section of gas molecules. According to the collision cross section data, the corresponding parameters can be calculated, and the critical breakdown field strength can be obtained from the ionization coefficient and the attachment coefficient. At present, the data of the collision cross section of gas are limited and are constantly replenished and improved. It is difficult to measure and calculate the collision cross section, which is an important factor that hinders the new gas research. The current micro-parameter calculations are based on some assumptions and simplifications. There is still a need for further research and exploration on the microscopic calculation of gas discharge to macroscopic processes.

(2) Extinguishing performance: Gas arc performance can be obtained through the interruption test in the laboratory or the circuit breaker equipment. By optimizing the structure of the arc extinguishing device, changing the size of the contact, and adding solid insulating materials, the gas arc extinguishing effect can be improved. According to the data in Table IV, it can be seen that there is not any arc-extinguishing medium, so looking for gases with excellent interruption performance is still the difficult point at present.

For the calculation of the arc extinguishing performance, the calculation of the arc conductance through thermodynamic performance, transport parameters, and radiation has been a relatively mature process. However, the calculation process is still in an ideal condition. The details of the calculation are still worth exploring. For example, the difference between the electron temperature and the heavy ion temperature in Non Local Thermodynamic Equilibrium (NLTE) and various particles of the chemical reaction rate in non-chemical equilibrium need to be considered in the calculation of equilibrium composition. In-depth exploration of the theory is still a research direction.

(3) For decomposition performance: The decomposition products of various gases in different discharge conditions can be measured by the experiment. However, for the theoretical calculation, at present, only the possible reaction path can be specified to calculate the reaction energy, and the calculations have some subjectivity. The chemical process is not calculated on the physical conditions, so the rate of formation of decomposition products cannot be calculated quantitatively according to the experimental conditions of discharge.

So far, SF_6 is still the most stable and reliable insulation and interrupter medium. The existing alternative gas as an insulation medium can be used in different equipment. In contrast, the interrupter medium needs further exploration. The new gas is still in constant exploration.

The gas-insulated medium is not a single kind of gas. Different gases may be used as the insulating medium in different equipment. Because there is no single insulating gas that can completely replace the use of SF_6 in electrical equipment, mixed gases have become the mainstream of development. There are still many unexplored areas for the gas currently studied. The molecular structure of the ideal alternative gas by computational chemistry can be designed. The calculation can predict the boiling point, insulation properties, and other aspects of the new insulating gas, which is a way to look for alternative gases.

At present, there is still no gas that can substitute for SF_6 completely, and the gas with good insulating property needs to be mixed with the buffer gas (except HFO1234zeE and CF_3I, which can be used alone as an insulating medium in the MV equipment). A series of problems (such as the leakage, the supplementary gas, the recovery, and the decomposition) brought by the use of the mixed gas need to be considered in the future, and the relevant industries are still being explored. Research on alternative gases still faces greater challenges and requires significant time and economic investment.

ACKNOWLEDGMENTS

This work was supported by the Natural Science Foundation of China (Program No. 51707137).

APPENDIX

Tables V–VIII contain the current research conclusions and references of major environmentally friendly gases.

REFERENCES

[1] H. Moissan and P. Lebeau, Compt. Rend. **130**, 869 (1900).

[2] G. Camilli and J. J. Chapman, "Gaseous insulation for high-voltage apparatus," Trans. Am. Inst. Electr. Eng. **66**(1), 1463–1470 (1947).

[3] G. Camilli, G. S. Gordon, and R. E. Plump, "Gaseous insulation for high-voltage transformers," Trans. Am. Inst. Electr. Eng., Part 3 **71**(1), 348–357 (1952).

[4] S. Menju, H. Aoyagi, K. Takahashi, and H. Qhno, "Dielectric breakdown of high pressure SF_6 in sphere and coaxial cylinder gaps," IEEE Trans. Power Appar. Syst. **PAS-93**(5), 1706–1712 (1974).

[5] S. Menju and K. Takahashi, "DC dielectric strength of a SF_6 gas insulated system," IEEE Trans. Power Appar. Syst. **PAS-97**, 217–224 (1978).

[6] F. A. M. Rizk, C. Masetti, and R. P. Comsa, "Particle-initiated breakdown in SF_6 insulated systems under high direct voltage," IEEE Trans. Power Appar. Syst. **PAS-98**(3), 825–836 (1979).

[7] H. A. Boyd and G. C. Crichton, "Measurement of ionisation and attachment coefficients in SF_6," Proc. Inst. Electr. Eng. **118**(12), 1872–1877 (1971).

[8] D. Berg and C. N. Works, "Temperature effect in the electrical breakdown of SF_6," in *1957 Conference on Electrical Insulation* (IEEE, 1957), p. 31.

[9] H. J. Lingal, A. P. Strom, and T. E. Browne, "An investigation of the arc-quenching behavior of sulfur hexafloride [includes discussion]," Trans. Am. Inst. Electr. Eng., Part 3 **72**(2), 242–246 (1953).

[10] C. F. Cromer and R. E. Friedrich, "A new 115-kv 1,000-mva gas-filled circuit breaker," Electr. Eng. **75**(12), 1085 (1956).

[11] W. M. Leeds, T. E. Browne, and A. P. Strom, "The use of SF_6 for high-power arc quenching," Electr. Eng. **76**(9), 788–791 (1957).

[12] R. Kane and R. Colclaser, "A 69-Kv SF_6 common-tank breaker rated 5,000 Mva," IEEE Trans. Power Appar. Syst. **82**(69), 1076–1082 (1963).

[13] G. J. Easley and J. M. Telford, "A new design 34.5 to 69 Kv intermediate capacity SF_6 circuit breaker," IEEE Trans. Power Appar. Syst. **83**(12), 1172–1177 (1964).

[14] R. C. Van Sickle and R. N. Yeckley, "A 500-kV circuit breaker using SF_6 gas," IEEE Trans. Power Appar. Syst. **84**(10), 892–901 (1965).

[15] C. F. Sonnenberg and J. J. Brado, "Insulation coordination qualities of 500-kV SF_6 circuit breakers," IEEE Trans. Power Appar. Syst. **84**(10), 851–863 (1965).

[16] R. Yeckley and C. Cromer, "New SF_6 EHV Circuit breakers for 550 kV and 765 kV," IEEE Trans. Power Appar. Syst. **PAS-89**(8), 2015–2023 (1970).

[17] R. Kane, R. Newsome, and C. Wagner, "New generation of oilless circuit breakers 115 kV-345kV I. System requirements," IEEE Trans. Power Appar. Syst. **PAS-90**(2), 628–635 (1971).

[18] E. Kane and Z. Neri, "New generation of oilless circuit breakers 115 kV-345kV III.-Insulation systems," IEEE Trans. Power Appar. Syst. **PAS-90**(2), 647–651 (1971).

[19] R. Crookston, W. Fischer, and R. Kane, "New generation of oilless circuit breakers 115 kV-345kV IV-The mechanical system," IEEE Trans. Power Appar. Syst. **PAS-90**(2), 652–659 (1971).

[20] T. F. Garrity, R. Matulic, and G. Rhodes, "Installation and field testing of 138kV SF_6 gas insulated station and transmission line," IEEE Trans. Power Appar. Syst. **94**(5), 1589–1598 (1975).

[21] L. Berkebile, C. Cromer, R. Kane, and F. Reese, "New generation of oilless circuit breakers 115 kV-345kV II-The interrupting system," IEEE Trans. Power Appar. Syst. **PAS-90**(2), 636–646 (1971).

[22] F. S. Cooper, U.S. Patent No. 2,221,671, U.S. Patent and Trademark Office, Washington, DC (12 November 1940).

[23] P. Parvopassu, F. Solimando, L. M. Rolandin, and E. Occhini, "150 kV EPM cable connections between transformers and SF_6 insulated switchgear for 5 substations in Rome," IEEE Trans. Power Appar. Syst. **96**(1), 178–183 (1977).

[24] K. Morii, S. Matsumura, T. Ushio, S. Tominaga, and Y. Shinozaki, "SF_6 gas circuit breaker, new solution for generator main circuit switching," IEEE Trans. Power Appar. Syst. **PAS-98**(3), 759–769 (1979).

[25] P. Bolin, A. Cookson, P. Kommineni, and K. Yoon, "Mechanical design and test of 1200 kV semi-flexible SF6 insulated transmission line," IEEE Trans. Power Appar. Syst. **PAS-101**(6), 1630–1637 (1982).

[26] Y. Harumoto, Y. Kabayama, Y. Kuroda, Y. Yoshida, H. Kan, Y. Miura, E. Tamaki, and T. Hakata, "Development of 275 kV EHV class gas-insulated power transformer," IEEE Trans. Power Appar. Syst. **PAS-104**(9), 2501–2508 (1985).

[27] S. P. Walldorf and P. A. Gnadt, "Development of 1200-kV compressed-gas-insulated transmission and substation equipment in the United States," IEEE Trans. Power Delivery **2**(2), 374–383 (1987).

[28] J.-y. Koo, J.-g. Seong, J.-s. Hwang, B.-w. Lee, and S.-h. Lee, "Design of 154 kV extra-high-voltage prototype SF6 bushing for superconducting electric power applications," Jpn. J. Appl. Phys., Part 1 **51**(9S2), 09ME01 (2012).

[29] T. R. Bjørtuft, E. Attar, M. Saxegaard, A. Sitko, O. Granhaug, and H. Landsverk, "Dielectric and thermal challenges for next generation ring main units (RMU)," 22nd International Conference on Electricity Distribution Stockholm, 10–13 June 2013, Paper 0463.

[30] D. Koch, SF6 Properties, and Use in MV and HV Switchgear, Cahier Technique, 2003, p. 188.

[31] X. Zhang, H. Xiao, J. Tang, Z. Cui, and Y. Zhang, "Recent advances in decomposition of the most potent greenhouse gas SF_6," Crit. Rev. Environ. Sci. Technol. **47**(18), 1763–1782 (2017).

[32] J. Devins, "Replacement gases for SF_6," IEEE Trans. Electr. Insul. **EI-15**(2), 81–86 (1980).

[33] S. Wock, "On the toxicity of SF_6 insulating gas," IEEE Trans. Electr. Insul. **EI-19**(2), 156 (1984).

[34] A. Vanroggen, P. F. Pugh, and K. P. Brand, "On the toxicity of SF_6 insulating gas," IEEE Trans. Electr. Insul. **E1-18**(1), 93 (1983).

[35] A. Vijk, "The nature of metal-electrodes/SF_6 reactions in SF_6 decomposition due to direct-current interruption under simulated circuit-breaker conditions," IEEE Trans. Electr. Insul. **EI-11**(4), 157–160 (1976).

[36] A. Kraut and R. Lilis, "Pulmonary effects of acute exposure to degradation products of sulphur hexafluoride during electrical cable repair work," Occup. Environ. Med. **47**(12), 829–832 (1990).

[37] K. J. Pilling and H. W. Jones, "Inhalation of degraded sulphur hexafluoride resulting in pulmonary oedema," Occup. Med. **38**(3), 82–84 (1988).

[38] C. Liu, S. Palanisamy, S. Chen, P. Wu, L. Yao, and B. S. Lou, "Mechanism of formation of SF_6 decomposition gas products and its identification by GC-MS and electrochemical methods: A mini review," Int. J. Electrochem. Sci. **10**(5), 4223–4231 (2015).

[39] G. D. Griffin, M. G. Nolan, C. E. Easterly, I. Sauers, and P. C. Votaw, "Concerning biological effects of spark-decomposed SF_6," IEE Proc., Part A: Phys. Sci., Meas. Instrum., Manage. Educ. **137**(4), 221–227 (1990).

[40] F. Jakob and M. B. A. Nicholas Perjanik, Sulfur hexafluoride: A unique dielectric, Analytical ChemTech International, Inc., 1998.

[41] B. Obama, "The irreversible momentum of clean energy," Science **355**(6321), 126–129 (2017).

[42]M. Grubb, C. Vrolijk, and D. Brack, *The Kyoto Protocol: A Guide and Assessment* (Royal Institute of International Affairs Energy and Environmental Programme, 1997).
[43]S. Xiao, "Research on insulation performance of SF_6 substitute CF_3I/CO_2 under power frequency voltage and the influence of micro-moisture on CF_3I," Ph.D. dissertation (Université de Toulouse, Université Toulouse III-Paul Sabatier, 2016).
[44]P. Purohit and L. Hoglund-Isaksson, "Global emissions of fluorinated greenhouse gases until 2050: Technical mitigation potentials and costs," in *EGU General Assembly Conference Abstracts* (EGU, 2016), Vol. 18.
[45]S. Xiao, X. Zhang, J. Tang, and S. Liu, "A review on SF_6 substitute gases and research status of CF_3I gases," J. Energy Rep. **4**, 523–535 (2018).
[46]J. D. Mantilla, N. Gariboldi, S. Grob, and M. Claessens, "Investigation of the insulation performance of a new gas mixture with extremely low GWP," in *2014 IEEE Electrical Insulation Conference (EIC)* (IEEE, 2014), pp. 469–473.
[47]Y. Kieffel, F. Biquez, and P. Ponchon, Alternative Gas to SF6 for Use in High Voltage Switchgears: G3, CIRED Paper No. 230, 2015.
[48]R. Ullah, A. Rashid, A. Rashid, F. Khan, and A. Ali, "Dielectric characteristic of dichlorodifluoromethane (R12) gas and mixture with N_2/air as an alternative to SF_6 gas," High Voltage **2**(3), 205–210 (2017).
[49]M. Koch and C. M. Franck, "High voltage insulation properties of HFO1234ze," IEEE Trans. Dielectr. Electr. Insul. **22**(6), 3260–3268 (2015).
[50]A. Beroual and A. Haddad, "Recent advances in the quest for a new insulation gas with a low impact on the environment to replace sulfur hexafluoride (SF_6) gas in high-voltage power network applications," Energies **10**(8), 1216 (2017).
[51]L. C. Zhang, *Study on Insulation Characteristics of c-C_4F_8 and its Gas Mixtures Substituting SF_6* (Shanghai Jiao Tong University, Shanghai, China, 2007).
[52]D. A. Price, J. Lucas, and J. L. Moruzzi, "Ionization in oxygen-hydrogen mixtures," J. Phys. D: Appl. Phys. **5**(7), 1249 (1972).
[53]See http://www.lxcat.laplace.univ-tlse.fr for more information about collisions.
[54]M.-x. Hou, W.-g. Li, C.-y. Yuan, Y.-x. Yang, and J. Ouyang, "Breakdown characteristics of CF_4 and CF_4/N_2 hybrid gas in refrigeration temperature range," J. Cent. South Univ. **24**(4), 861–865 (2017).
[55]A. Banković, S. Dujko, S. Marjanović, R. D. White, and Z. L. Petrović, "Positron transport in CF_4 and N_2/CF_4 mixtures," Eur. Phys. J. D **68**(5), 127 (2014).
[56]H. Itoh, T. Matsumura, K. Satoh, H. Date, Y. Nakao, and H. Tagashira, "Electron transport coefficients in SF_6," J. Phys. D: Appl. Phys. **26**(11), 1975 (1993).
[57]M. J. Pinheiro and J. Loureiro, "Effective ionization coefficients and electron drift velocities in gas mixtures of SF_6 with He, Xe, CO_2 and N_2 from Boltzmann analysis," J. Phys. D: Appl. Phys. **35**(23), 3077 (2002).
[58]X. Yu, H. Hou, and B. Wang, "Prediction on dielectric strength and boiling point of gaseous molecules for replacement of SF_6," J. Comput. Chem. **38**(10), 721–729 (2017).
[59]O. Mayr, "Beiträge zur theorie des statischen und des dynamischen Lichtbogens," Arch. Elektrotech. **37**(12), 588–608 (1943).
[60]G. Yang and J. Heberlein, "Anode attachment modes and their formation in a high intensity argon arc," Plasma Sources Sci. Technol. **16**(3), 529 (2007).
[61]T. Amakawa, J. Jenista, J. Heberlein, and E. Pfender, "Anode-boundary-layer behaviour in a transferred, high-intensity arc," J. Phys. D: Appl. Phys. **31**(20), 2826 (1998).
[62]R. G. Parr, "Density functional theory," Annu. Rev. Phys. Chem. **34**(1), 631–656 (1983).
[63]A. Gleizes, J. J. Gonzalez, and P. Freton, "Thermal plasma modelling," J. Phys. D: Appl. Phys. **38**(9), R153 (2005).
[64]A. B. Murphy, "Thermal plasmas in gas mixtures," J. Phys. D: Appl. Phys. **34**(20), R151 (2001).
[65]W. Z. Wang, M. Z. Rong, J. D. Yan, A. B. Murphy, and J. W. Spencer, "Thermophysical properties of nitrogen plasmas under thermal equilibrium and non-equilibrium conditions," Phys. Plasmas **18**(11), 113502 (2011).
[66]X. Zhang, J. Zhang, Y. Jia, P. Xiao, and J. Tang, "TiO_2 nanotube array sensor for detecting the SF_6 decomposition product SO_2," Sensors **12**(3), 3302–3313 (2012).
[67]J. Tang, F. Liu, Q. Meng, X. Zhang, and J. Tao, "Partial discharge recognition through an analysis of SF_6 decomposition products part 2: Feature extraction and decision tree-based pattern recognition," IEEE Trans. Dielectr. Electr. Insul. **19**(1), 37–44 (2012).
[68]J. Tang, C. J. Chen, X. X. Zhang, F. Liu, and X. L. Ren, "Influence of trace-level O_2 on SF_6 decomposition characteristics under partial discharge," Gaodianya Jishu/ High Voltage Eng. **37**(1), 8–14 (2011).
[69]X.-x. Zhang, W.-t. Liu, J. Tang, and P. Xiao, "Study on PD detection in SF_6 using multi-wall carbon nanotube films sensor," IEEE Trans. Dielectr. Electr. Insul. **17**(3), 833–838 (2010).
[70]S. Xiao, X. Zhang, J. Tang, F. Zeng, C. Pan, and Y. Gui, "Comparative study of materials to SF_6 decomposition components," in *Nanomaterials Based Gas Sensors for SF_6 Decomposition Components Detection* (IntechOpen, 2017).
[71]X. Zhang, H. Zhou, C. Chen, X. Li, Z. Cui, S. Xiao, and J. Tang, "Ultraviolet differential optical absorption spectrometry: Quantitative analysis of the CS_2 produced by SF_6 decomposition," Meas. Sci. Technol. **28**(11), 115102 (2017).
[72]X. Zhang, Y. Gui, and Z. Dai, "Adsorption of gases from SF_6 decomposition on aluminum-doped SWCNTs: A density functional theory study," Eur. Phys. J. D **69**(7), 185 (2015).
[73]F. Zeng, J. Tang, X. Zhang, J. Pan, Q. Yao, and X. Hou, "Influence regularity of trace H_2O on SF_6 decomposition characteristics under partial discharge of needle-plate electrode," IEEE Trans. Dielectr. Electr. Insul. **22**(1), 287–295 (2015).
[74]J. Tang, F. Zeng, X. Zhang, J. Pan, Q. Yao, X. Hou, and Y. Tang, "Relationship between decomposition gas ratios and partial discharge energy in GIS, and the influence of residual water and oxygen," IEEE Trans. Dielectr. Electr. Insul. **21**(3), 1226–1234 (2014).
[75]F. Zeng, J. Luo, J. Tang, Q. Zhou, and Q. Yao, "Influence regularity of aluminum, copper and stainless-steel on SF_6 PD decomposition characteristics components," J. Electr. Eng. Technol. **12**(1), 295–301 (2017).
[76]J. Tang, Z. Cao, F. Zeng, Q. Yao, Y. Miao, and N. Qiu, "Influence of metallic materials on SF_6 decomposition components under positive DC partial discharge," Plasma Chem. Plasma Process. **37**(6), 1523–1534 (2017).
[77]Y. Fu, M. Rong, K. Yang, A. Yang, X. Wang, Q. Gao, D. Liu, and A. B. Murphy, "Calculated rate constants of the chemical reactions involving the main byproducts SO_2F, SOF_2, SO_2F_2 of SF_6 decomposition in power equipment," J. Phys. D: Appl. Phys. **49**(15), 155502 (2016).
[78]F. Zeng, J. Tang, Q. Fan, J. Pan, X. Zhang, Q. Yao, and J. He, "Decomposition characteristics of SF_6 under thermal fault for temperatures below 400 C," IEEE Trans. Dielectr. Electr. Insul. **21**(3), 995–1004 (2014).
[79]X. Zhang, S. Tian, S. Xiao, Z. Deng, Y. Li, and J. Tang, "Insulation strength and decomposition characteristics of a $C_6F_{12}O$ and N_2 gas mixture," Energies **10**(8), 1170 (2017).
[80]E. Husain and R. S. Nema, "Analysis of Paschen curves for air, N_2 and SF_6 using the Townsend breakdown equation," IEEE Trans. Electr. Insul. **EI-17**(4), 350–353 (1982).
[81]M. Hara, K. Adachi, H. Tobata, M. Akazaki, and F. L. Mao, "Particle-initiated breakdown characteristics of conical insulator in N_2 gas and N_2/O_2 mixture under DC voltage," IEEE Trans. Electr. Insul. **EI-22**(1), 87–96 (1987).
[82]T. Mizuno, K. Morita, Y. Kurata, and H. Miyagawa, "The electrical performance of air or nitrogen gas with solid insulation and the application for switchgears," in *IEEE/PES Transmission and Distribution Conference and Exhibition* (IEEE, 2002), Vol. 3, pp. 1797–1801.
[83]S. Philp, "Compressed gas insulation in the million-volt range: A comparison or SF_6 with N_2 and CO_2," IEEE Trans. Power Appar. Syst. **82**(66), 356–359 (1963).
[84]S. Meijer, J. J. Smit, and A. Girodet, "Comparison of the breakdown strength of N_2, CO_2 and SF_6 using the extended up-and-down method," in *2006 IEEE 8th International Conference on Properties* & *applications of Dielectric Materials* (IEEE, 2006), pp. 653–656.
[85]G. Ueta, J. Wada, and S. Okabe, "Evaluation of breakdown characteristics of CO_2 gas for non-standard lightning impulse waveforms-method for converting non-standard lightning impulse waveforms into standard lightning impulse waveforms," IEEE Trans. Dielectr. Electr. Insul. **18**(5), 1724–1733 (2011).
[86]J. Wada, G. Ueta, and S. Okabe, "Evaluation of breakdown characteristics of CO_2 gas for non-standard lightning impulse waveforms-breakdown characteristics in the presence of bias voltages under non-uniform electric field," IEEE Trans. Dielectr. Electr. Insul. **20**(1), 112–121 (2013).

[87] J. Wada, G. Ueta, and S. Okabe, "Evaluation of breakdown characteristics of N_2 gas for non-standard lightning impulse waveforms-breakdown characteristics under single-frequency oscillation waveforms and with bias voltages," IEEE Trans. Dielectr. Electr. Insul. **18**(5), 1759–1766 (2011).

[88] W. Pfeiffer and D. Schoen, "Prebreakdown phenomena in 20/80% N_2O/N_2 gas mixtures for vft-voltage stress," in *Proceedings of the XV International Conference on Gas Discharges and their Applications* (GD, 2004), pp. 359–362.

[89] J. M. Pelletier, Y. Gervais, and D. Mukhedkar, "Dielectric strength of N_2-He mixtures and comparison with N_2-SF_6 and CO_2-SF_6 mixtures," IEEE Trans. Power Appar. Syst. **PAS-100**(8), 3861–3869 (1981).

[90] D.-Y. Lim and S. Bae, "Study on oxygen/nitrogen gas mixtures for the surface insulation performance in gas insulated switchgear," IEEE Trans. Dielectr. Electr. Insul. **22**(3), 1567–1576 (2015).

[91] T. Rokunohe, Y. Yagihashi, F. Endo, and T. Oomori, "Fundamental insulation characteristics of air; N_2, CO_2, N_2/O_2, and SF_6/N_2 mixed gases," Electr. Eng. Jpn. **155**(3), 9–17 (2006).

[92] F. Pontiga and A. Castellanos, "Nitrogen oxides generation induced by negative corona discharge in N_2+O_2 mixtures," in *2006 IEEE Conference on Electrical Insulation and Dielectric Phenomena* (IEEE, 2006), pp. 264–267.

[93] H. Saitoh, K. Morita, T. Kikkawa, N. Hayakawa, and H. Okubo, "Impulse partial discharge and breakdown characteristics of rod–plane gaps in air and N_2 gases," Electr. Eng. Jpn. **148**(3), 36–43 (2004).

[94] H. Goshima, H. Shinkai, and M. Yashima, "Lightning impulse breakdown characteristics of high-pressure N_2 as an alternative insulation gas to SF_6," in *Gaseous Dielectrics IX* (Springer, Boston, MA, 2001), pp. 359–364.

[95] Q. H. Zhang, Y. Tan, and J. G. Wu, "40.5 kV non SF6 C-GIS research," in *2011 1st International Conference on Electric Power Equipment-Switching Technology* (IEEE, 2011), pp. 172–177.

[96] H. Zhao, X. Li, S. Jia, and A. B. Murphy, "Prediction of the critical reduced electric field strength for carbon dioxide and its mixtures with 50% O_2 and 50% H_2 from Boltzmann analysis for gas temperatures up to 3500 K at atmospheric pressure," J. Phys. D: Appl. Phys. **47**(32), 325203 (2014).

[97] H. Zhao, Y. Deng, and H. Lin, "Study of the synergistic effect in dielectric breakdown property of CO_2–O_2 mixtures," AIP Adv. **7**(9), 095102 (2017).

[98] Z. Chen, C. Niu, H. Zhang, H. Sun, Y. Wu, F. Yang, M. Rang, and Z. Xu, "Investigation on the reduced critical breakdown field of hot CO_2 gas and CO_2-based mixtures," in *2015 3rd International Conference on Electric Power Equipment–Switching Technology (ICEPE-ST)* (IEEE, 2015), pp. 36–39.

[99] M. Yousfi, J. de Urquijo, A. Juarez, E. Basurto, and J. L. Hernandez-Avila, "Electron swarm coefficients in CO_2-N_2 and CO_2-O_2 mixtures," IEEE Trans. Plasma Sci. **37**(6), 764–772 (2009).

[100] J. L. Moruzzi and D. A. Price, "Ionization, attachment and detachment in air and air-CO_2 mixtures," J. Phys. D: Appl. Phys. **7**(10), 1434 (1974).

[101] G. R. G. Raju and G. R. Gurumurthy, "Electron transport coefficients in N_2 in crossed fields at low E/p," IEEE Trans. Plasma Sci. **4**(4), 241–245 (1976).

[102] H. N. Kucukarpaci and J. Lucas, "Simulation of electron swarm parameters in carbon dioxide and nitrogen for high E/N," J. Phys. D: Appl. Phys. **12**(12), 2123 (1979).

[103] P. C. Stoller, M. Seeger, A. A. Iordanidis, and G. V. Naidis, "CO_2 as an arc interruption medium in gas circuit breakers," IEEE Trans. Plasma Sci. **41**(8), 2359–2369 (2013).

[104] E. Jonsson, N. S. Aanensen, and M. Runde, "Current interruption in air for a medium-voltage load break switch," IEEE Trans. Power Delivery **29**(2), 870–875 (2014).

[105] N. S. Aanensen, E. Jonsson, and M. Runde, "Air-flow investigation for a medium-voltage load break switch," IEEE Trans. Power Delivery **30**(1), 299–306 (2015).

[106] E. Jonsson and M. Runde, "Interruption in air for different medium-voltage switching duties," IEEE Trans. Power Delivery **30**(1), 161–166 (2015).

[107] N. S. Stoa-Aanensen, M. Runde, E. Jonsson, and A. D. O. Teigset, "Empirical relationships between air-load break switch parameters and interrupting performance," IEEE Trans. Power Delivery **31**(1), 278–285 (2016).

[108] T. Uchii, T. Shinkai, and K. Suzuki, "Thermal interruption capability of carbon dioxide in a puffer-type circuit breaker utilizing polymer ablation," in *IEEE/PES Transmission and Distribution Conference and Exhibition* (IEEE, 2002), Vol. 3, pp. 1750–1754.

[109] Z. Q. Chen, X. Cheng, L. Y. Jiao, and G. W. Ge, "Simulation on the high current interruption principle for hybrid circuit breaker of vacuum interrupter and CO_2 gas interrupter," in *2016 27th International Symposium on Discharges and Electrical Insulation in Vacuum (ISDEIV)* (IEEE, 2016), Vol. 2, pp. 1–4.

[110] X. Cheng, Z. Chen, G. Ge, Y. Wang, M. Liao, and L. Jiao, "Dynamic dielectric recovery synergy of hybrid circuit breaker with CO_2 gas and vacuum interrupters in series," IEEE Trans. Plasma Sci. **45**(10), 2885–2892 (2017).

[111] T. Matsumura, Y. Yokomizu, D. Kanda, T. Kumazawa, T. Furuhata, and K. Mitsukuchi, "Effect of magnetic field strength and admixture gas on current interrupting capability of a CO_2 rotary-arc load-break switch," Electr. Eng. Jpn. **167**(2), 21–27 (2009).

[112] L. Zhong, X. Wang, M. Rong, and Y. Cressault, "Effects of copper vapour on thermophysical properties of CO_2-N_2 plasma," Eur. Phys. J. D **70**(11), 233 (2016).

[113] N. Malik and A. Qureshi, "A review of electrical breakdown in mixtures of SF_6 and other gases," IEEE Trans. Electr. Insul. **EI-14**(1), 1–13 (1979).

[114] N. Malik and A. Qureshi, "Calculation of discharge inception voltages in SF_6-N_2 mixtures," IEEE Trans. Electr. Insul. **EI-14**(2), 70–76 (1979).

[115] A. Yializis, N. H. Malik, A. H. Qureshi, and E. Kuffel, "Impulse breakdown and corona characteristics for rod-plane gaps in mixtures of SF_6 and nitrogen with less than 1% of SF_6 content," IEEE Trans. Power Appar. Syst. **PAS-98**(5), 1832–1840 (1979).

[116] O. Farish, O. E. Ibrahim, and B. H. Crichton, "Effect of electrode surface roughness on breakdown in nitrogen/SF_6 mixtures," Proc. Inst. Electr. Eng. **123**(10), 1047–1050 (1976).

[117] R. Graf and W. Boeck, "Defect sensibility of N_2-SF_6 gas mixtures with equal dielectric strength," in *2000 Annual Report Conference on Electrical Insulation and Dielectric Phenomena (Cat. No. 00CH37132)* (IEEE, 2000), Vol. 1, pp. 422–425.

[118] S.-Y. Woo, D.-H. Jeong, K.-B. Seo, and J.-H. Kim, "A study on dielectric strength and Insulation property of SF_6/N_2 mixtures for GIS," J. Int. Council Electr. Eng. **2**(1), 104–109 (2012).

[119] M. A. Guerroui and A. Lemzadmi, "Polarity effect on corona discharge voltages in SF_6-N_2 gas mixtures," Eur. Sci. J. **9**(21), 72–75 (2013).

[120] H. Sato, K. Morita, T. Kikkawa, N. Hayakawa, and H. Okubo, "A fundamental study on electrical insulation of N_2/SF_6 gas-insulated electric power apparatus," Electr. Eng. Jpn. **139**(4), 9–16 (2002).

[121] Y. Hoshina, M. Sato, H. Murase, M. Toyada, and A. Kobayashi, "Dielectric properties of SF_6/N_2 gas mixtures on a full scale model of the gas-insulated busbar," in *2000 IEEE Power Engineering Society Winter Meeting. Conference Proceedings (Cat. No. 00CH37077)* (IEEE, 2000), Vol. 3, pp. 2129–2134.

[122] C. Guo, Q. Zhang, and T. Wen, "A method for synergistic effect evaluation of SF_6/N_2 gas mixtures," IEEE Trans. Dielectr. Electr. Insul. **23**(1), 211–215 (2016).

[123] F. Rizk and M. Eteiba, "Impulse breakdown voltage-time curves of SF_6 and SF_6-N_2 coaxial-cylinder gaps," IEEE Trans. Power Appar. Syst. **PAS-101**(12), 4460–4471 (1982).

[124] T. Mizobuchi, H. Toyota, S. Matsuoka, A. Kumada, and K. Hidaka, "Nanosecond electrical discharge development in SF_6-N_2 gas mixtures," IEEJ Trans. Fundam. Mater. **125**(8), 629–635 (2005).

[125] C. Jiasen, W. Hu, Z. Qiaogen, and Q. Aici, "Multichannel discharge characteristics of gas switch gap in SF_6-N_2 or SF_6-Ar gas mixtures under nanosecond triggering pulses," Plasma Sci. Technol. **13**(6), 719–723 (2011).

[126] T. Hirata, H. Ueno, and H. Nakayama, "Characteristics of N_2/SF_6 mixture gas in creeping discharge developing in narrow gap with backside electrode," Electr. Eng. Jpn. **158**(2), 31–38 (2007).

[127] H. Koch and M. Hopkins, "Overview of gas insulated lines (GIL)," in *IEEE Power Engineering Society General Meeting* (IEEE, 2005), pp. 940–944.

[128] N. H. Malik, A. H. Qureshi, and Y. A. Safar, "DC voltage breakdown of SF_6-air and SF_6-CO_2 mixtures in rod-plane gaps," IEEE Trans. Electr. Insul. **EI-18**(6), 629–636 (1983).

[129] Z. Li, R. Kuffel, and E. Kuffel, "Volt-time characteristics in air, SF_6/air mixture and N_2 for coaxial cylinder and rod-sphere gaps," IEEE Trans. Electr. Insul. **EI-21**(2), 151–155 (1986).

[130]Y. Qiu, S. Y. Chen, Y. F. Liu, and E. Kuffel, "Comparison of SF_6/N_2 and SF_6/CO_2 gas mixtures based on the figure-of-merit concept," in *Annual Report: Conference on Electrical Insulation and Dielectric Phenomena* (IEEE, 1988), pp. 299–304.
[131]Y. Qiu and E. Kuffel, "Comparison of SF_6/N_2 and SF_6/CO_2 gas mixtures as alternatives to SF_6 gas," IEEE Trans. Dielectr. Electr. Insul. **6**(6), 892–895 (1999).
[132]Y. Qiu and I. D. Chalmers, "Effect of electrode surface roughness on breakdown in SF_6-N_2 and SF_6-CO_2 gas mixtures," J. Phys. D: Appl. Phys. **26**(11), 1928 (1993).
[133]S. Ohtsuka, S. Nagara, M. Koumura, Y. Hashimoto, M. Nakamura, and M. Hikita, "Insulation properties of a CO_2/N_2 50% SF_6 gas mixture in a nonuniform field," Electr. Eng. Jpn. **140**(3), 34–43 (2002).
[134]Y. Safar, N. Malik, and A. Qureshi, "Impulse breakdown behavior of negative rod-plane gaps in SF_6-N_2, SF_6-air and SF_6-CO_2 mixtures," IEEE Trans. Electr. Insul. **EI-17**(5), 441–450 (1982).
[135]A. H. Cookson and R. E. Wootton, "AC corona and breakdown characteristics for rod gaps in compressed hydrogen, SF_6 and hydrogen-SF_6 mixtures," IEEE Trans. Power Appar. Syst. **PAS-97**(2), 415–423 (1978).
[136]O. Farish, S. J. Dale, and A. M. Sletten, "Impulse breakdown of negative rod-plane gaps in hydrogen and hydrogen-SF_6 mixtures," IEEE Trans. Power Appar. Syst. **PAS-97**(1), 118–124 (1978).
[137]M. Akbar and N. H. Malik, "Electrical breakdown of N_2O-SF_6, N_2O-CCL_2F_2 and N_2O-CO_2 gas mixtures," IEEE Trans. Electr. Insul. **EI-20**(3), 581–585 (1985).
[138]S. W. Park, C. H. Hwang, N. R. Kim, K. T. Lee, and C. S. Huh, "Breakdown characteristics of SF_6/CF_4 mixtures in test chamber and 25.8 kV GIS," Eng. Lett. **15**(1), 145–148 (2007).
[139]C. H. Hwang, B. T. Lee, C. S. Huh, N. R. Kim, and Y. M. Chang, "Breakdown characteristics of SF_6/CF_4 mixtures in 25.8 kV," in *2009 International Conference on Electrical Machines and Systems* (IEEE, 2009), pp. 1–4.
[140]J. M. Berg, *Experimental Studies of SF_6-CF_4 Mixtures for Use as Gaseous Dielectrics in Power System Applications* (The University of Manitoba, Manitoba, Canada, 1995).
[141]J. Berg and E. Kuffel, "Breakdown voltage characteristics of SF6/CF4 mixtures in uniform and non-uniform field gaps," in *Proceedings of 1995 Conference on Electrical Insulation and Dielectric Phenomena* (IEEE, 1995), pp. 126–129.
[142]K. Toufani, *Experimental Studies of Breakdown Characteristics of SF_6/CF_4 Mixtures in Highly Non-uniform Fields for High-Voltage Applications* (The University of Manitoba, Manitoba, Canada, 1997).
[143]S. H. Lee, J. K. Seong, S. H. Oh, W. J. Shin, U. A. Khan, and B. W. Lee, "Breakdown characteristics of liquefied and gases in liquid nitrogen for high voltage bushings in a cryogenic environment," IEEE Trans. Appl. Supercond. **21**(3), 1430–1433 (2011).
[144]M. Siddagangappa, C. Lakshminarasimha, and M. Naidu, "Prediction of breakdown voltages of binary gas mixtures in uniform electric fields," IEEE Trans. Electr. Insul. **EI-19**(4), 359–361 (1984).
[145]R. Nema, S. Kulkarni, and E. Husain, "Calculation of sparking potentials of SF_6 and SF_6-gas mixtures in uniform and non-uniform electric fields," IEEE Trans. Electr. Insul. **EI-17**(1), 70–75 (1982).
[146]V. N. Maller and M. S. Naidu, "Ionization and breakdown in SF_6-air and freon-nitrogen mixtures," IEEE Trans. Plasma Sci. **3**(2), 49–54 (1975).
[147]N. Malik and A. Qureshi, "Breakdown gradients in SF_6-N_2, SF_6-Air and SF_6-CO_2 mixtures," IEEE Trans. Electr. Insul. **EI-15**(5), 413–418 (1980).
[148]G. R. Govinda Raju and R. Hackam, "Breakdown field strength of SF_6, N_2O, SF_6+N_2, and SF_6+N_2O," J. Appl. Phys. **52**(6), 3912–3920 (1981).
[149]L. E. Kline, D. K. Davies, C. L. Chen, and P. J. Chantry, "Dielectric properties for SF_6 and SF_6 mixtures predicted from basic data," J. Appl. Phys. **50**(11), 6789–6796 (1979).
[150]M. S. Dincer and G. R. Govinda Raju, "Ionization and attachment coefficients in SF_6+N_2 mixtures," IEEE Trans. Electr. Insul. **EI-19**(1), 40–44 (1984).
[151]G. R. Govinda Raju and M. S. Dincer, "Measurement of ionization and attachment coefficients in SF_6 and SF_6+N_2," J. Appl. Phys. **53**(12), 8562–8567 (1982).
[152]Z. Y. Lee, "Measurements of breakdown potential and ionization and attachment in SF_6-CO_2 mixtures," IEEE Trans. Electr. Insul. **EI-18**(6), 637–641 (1983).
[153]M. F. Fréchette, "Experimental study of SF_6/N_2 and SF_6/CCl_2F_2 mixtures by the steady-state Townsend method," J. Appl. Phys. **59**(11), 3684–3693 (1986).
[154]A. V. Phelps and R. J. Van Brunt, "Electron-transport, ionization, attachment, and dissociation coefficients in SF_6 and its mixtures," J. Appl. Phys. **64**(9), 4269–4277 (1988).
[155]D. M. Xiao, X. G. Li, and X. Xu, "Swarm parameters in SF_6 and CO_2 gas mixtures," J. Phys. D: Appl. Phys. **34**(24), L133 (2001).
[156]J. L. Hernández-Ávila, E. Basurto, and J. de Urquijo, "Electron transport and swarm parameters in CO_2 and its mixtures with SF_6," J. Phys. D: Appl. Phys. **35**(18), 2264 (2002).
[157]J. de Urquijo, E. Basurto, and J. L. Hernández-Ávila, "Measurement of electron drift, diffusion, and effective ionization coefficients in the SF_6–CHF_3 and SF_6–CF_4 gas mixtures," J. Phys. D: Appl. Phys., Part 1 **36**(24), 3132 (2003).
[158]D. M. Xiao, J. L. Yang, and X. Xu, "Electron swarm parameters in SF_6 and CF_4 gas mixtures," Jpn. J. Appl. Phys., Part 2 **43**(3A), L369 (2004).
[159]X. Liu and D. Xiao, "Monte Carlo simulation of electron swarm parameters in the SF_6/CF_4 gas mixtures," Jpn. J. Appl. Phys., Part 1 **46**(4R), 1663 (2007).
[160]W. Feng, W. Pfeiffer, N. Kouzichine, Q. Yuchang, E. Kuffel, and L. Kenli, "Calculation of electron swarm parameters of SF_6/N_2 in a uniform field using an improved Monte Carlo collision simulation method," Plasma Sci. Technol. **10**(1), 39 (2008).
[161]H. Zhao, X. Li, S. Jia, and A. B. Murphy, "Dielectric breakdown properties of SF_6–N_2 mixtures at 0.01–1.6 MPa and 300–3000 K," J. Appl. Phys. **113**(14), 143301 (2013).
[162]X. Li, H. Zhao, S. Jia, and A. B. Murphy, "Study of the dielectric breakdown properties of hot SF_6–CF_4 mixtures at 0.01–1.6 MPa," J. Appl. Phys. **114**(5), 053302 (2013).
[163]L. Zhong, A. Yang, X. Wang, D. Liu, Y. Wu, and M. Rong, "Dielectric breakdown properties of hot SF_6-CO_2 mixtures at temperatures of 300–3500 K and pressures of 0.01–1.0 MPa," Phys. Plasmas **21**(5), 053506 (2014).
[164]A. V. Larin, N. Meurice, D. N. Trubnikov, and D. P. Vercauteren, "Theoretical analysis of the synergism in the dielectric strength for SF_6/CF_4 mixtures," J. Appl. Phys. **96**(1), 109–117 (2004).
[165]A. Lee and L. S. Frost, "Interruption capability of gases and gas mixtures in a puffer-type interrupter," IEEE Trans. Plasma Sci. **8**(4), 362–367 (1980).
[166]K. Tomita, D. Gojima, K. Nagai, K. Uchino, R. Kamimae, Y. Tanaka, K. Suzuki, T. Iijima, T. Uchii, and T. Shinkai, "Thomson scattering diagnostics of decay processes of Ar/SF_6 gas-blast arcs confined by a nozzle," J. Phys. D: Appl. Phys. **46**(38), 382001 (2013).
[167]A. Gleizes, M. Razafinimanana, and S. Vacquie, "Transport coefficients in arc plasma of SF_6–N_2 mixtures," J. Appl. Phys. **54**(7), 3777–3787 (1983).
[168]B. Chervy, H. Riad, and A. Gleizes, "Calculation of the interruption capability of SF_6-CF_4 and SF_6-C_2F_6 mixtures. I. Plasma properties," IEEE Trans. Plasma Sci. **24**(1), 198–209 (1996).
[169]B. Chervy, J.-J. Gonzalez, and A. Gleizes, "Calculation of the interruption capability of SF_6-CF_4 and SF_6-C_2F_6 mixtures-Part II: Arc decay modeling," IEEE Trans. Plasma Sci. **24**(1), 210–217 (1996).
[170]W. Wang, M. Rong, Y. Wu, and J. D. Yan, "Fundamental properties of high-temperature SF_6 mixed with CO_2 as a replacement for SF_6 in high-voltage circuit breakers," J. Phys. D: Appl. Phys. **47**(25), 255201 (2014).
[171]W. Wang, X. Tu, D. Mei, and M. Rong, "Dielectric breakdown properties of hot SF_6/He mixtures predicted from basic data," Phys. Plasmas **20**(11), 113503 (2013).
[172]R. L. Middleton and P. Eng, "Cold-weather application of gas mixture (SF_6/N_2, SF_6/CF_4) circuit breakers: A utility user's perspective," in 1st Conference on SF6 and Environment: Emission and Reduction Strategies, November 2000.
[173]F. Yang, Z. Chen, Y. Wu, M. Rong, A. Guo, Z. Liu, and C. Wang, "Two-temperature transport coefficients of SF_6-N_2 plasma," Phys. Plasmas **22**(10), 103508 (2015).
[174]H. Zhao, X. Li, K. Zhu, Q. Wang, H. Lin, and X. Guo, "Study of the arc interruption performance of SF_6-CO_2 mixtures as a substitute for SF 6," IEEE Trans. Dielectr. Electr. Insul. **23**(5), 2657–2667 (2016).
[175]C. Pradayrol, A. M. Casanovas, A. Hernoune, and J. Casanovas, "Spark decomposition of and mixtures," J. Phys. D: Appl. Phys. **29**(7), 1941 (1996).

[176] A. M. Casanovas, I. Coll, C. Pradayrol, and J. Casanovas, "Influence of a solid insulator on the spark decomposition of SF_6 and 50%SF_6+50%CF_4 mixtures," J. Phys. D: Appl. Phys. **31**(20), 2835 (1998).
[177] C. Pradayrol, A. M. Casanovas, C. Aventin, and J. Casanovas, "Production of SO_2F_2, SOF_4, (SOF_2 + SF_4), S_2F_{10}, S_2OF_{10} and S_2O_2F10 in SF_6 and (50–50) SF_6–CF_4 mixtures exposed to negative coronas," J. Phys. D: Appl. Phys. **30**(9), 1356 (1997).
[178] I. Sauers, "By-product formation in spark breakdown of SF_6/O_2 mixtures," Plasma Chem. Plasma Process. **8**(2), 247–262 (1988).
[179] L. Vial, A. M. Casanovas, I. Coll, and J. Casanovas, "Decomposition products from negative and 50 Hz AC corona discharges in compressed SF_6 and SF_6/N_2 (10: 90) mixtures. Effect of water vapour added to the gas," J. Phys. D: Appl. Phys. **32**(14), 1681 (1999).
[180] L. Vial, A. M. Casanovas, J. Diaz, I. Coll, and J. Casanovas, "Decomposition of high-pressure (400 kPa) SF_6 and SF_6/N_2 (10: 90) mixtures submitted to negative or 50 Hz ac corona discharges in the presence of water vapour and/or oxygen," J. Phys. D: Appl. Phys. **34**(13), 2037 (2001).
[181] I. Coll, A. M. Casanovas, L. Vial, A. Gleizes, and J. Casanovas, "Sparking-induced decomposition of 10% SF_6-90% N_2 mixtures: Effect of a solid organic insulator, oxygen and water," J. Phys. D: Appl. Phys. **33**(11), 1348 (2000).
[182] A. M. Casanovas and J. Casanovas, "Decomposition of high-pressure (400 kPa) SF_6-CO_2, SF_6-CO, SF_6-N_2-CO_2 and SF_6-N_2-CO mixtures under negative dc coronas," J. Phys. D: Appl. Phys. **38**(10), 1556 (2005).
[183] W. Liu, Z. Su, J. Qi, F. Zhu, Y. Zhao, F. Ma, X. Yuan, and Y. Chen, "Application and recycling of SF_6 gas mixtures in gas-insulated circuit breaker in northern China," IOP Conf. Ser.: Earth Environ. Sci. **69**(1), 012002 (2017).
[184] I. Cha, S. Lee, J. D. Lee, G.-w. Lee, and Y. Seo, "Separation of SF_6 from gas mixtures using gas hydrate formation," Environ. Sci. Technol. **44**(16), 6117–6122 (2010).
[185] L. Niemeyer, "Cigre guide for SF_6 gas mixtures: Application and handling in electric power equipment," in *Proceedings of the 1st Conference on SF_6 and Environment: Emission and Reduction Strategies* (CIGRE, 2000), pp. 2–3.
[186] T. Takuma, S. Hamada, and O. Yamamoto, "Application of a gas mixture with c-C_4F_8 in gas insulation," in *1999 Eleventh International Symposium on High Voltage Engineering* (IET, 1999), Vol. 3, pp. 197–200.
[187] J. Wada, G. Ueta, S. Okabe, and M. Hikita, "Dielectric properties of gas mixtures with per-fluorocarbon gas and gas with low liquefaction temperature," IEEE Trans. Dielectr. Electr. Insul. **23**(2), 838–847 (2016).
[188] S. Zhao, J. Jiao, X. Zhao, H. Zhang, D. Xiao, and J. D. Yan, "Synergistic effect of c-C_4F_8/N_2 gas mixtures in slightly non-uniform electric field under lightning impulse," in *2016 IEEE Electrical Insulation Conference (EIC)* (IEEE, 2016), pp. 531–534.
[189] L. Whitman, "Impulse voltage tests on air and C_3F_8," IEEE Trans. Electr. Insul. **EI-1**(2), 44–48 (1965).
[190] H. Okubo, T. Yamada, K. Hatta, N. Hayakawa, S. Yuasa, and S. Okabe, "Partial discharge and breakdown mechanisms in ultra-dilute SF_6 and PFC gases mixed with N_2 gas," J. Phys. D: Appl. Phys. **35**(21), 2760 (2002).
[191] J. de Urquijo and E. Basurto, "Electron attachment, ionization and drift in c-C_4F_8," J. Phys. D: Appl. Phys. **34**(9), 1352 (2001).
[192] H. Itoh, T. Miyachi, M. Kawaguchi, Y. Nakao, and H. Tagashira, "Electron transport coefficients in SF_6 and c-C_4F_8 mixtures," J. Phys. D: Appl. Phys. **24**(3), 277 (1991).
[193] B.-T. Wu, D.-M. Xiao, Z.-S. Liu, L.-C. Zhang, and X.-L. Liu, "Analysis of insulation characteristics of c-C_4F_8 and N_2 gas mixtures by the Monte Carlo method," J. Phys. D: Appl. Phys. **39**(19), 4204 (2006).
[194] X. Liu, J. Wang, Y. Wang, Z. Zhang, and D. Xiao, "Analysis of the insulation characteristics of c-C_4F_8/CO_2 gas mixtures by the Monte Carlo method," J. Phys. D: Appl. Phys. **41**(1), 015206 (2007).
[195] X. Li, H. Zhao, S. Jia, and A. B. Murphy, "Prediction of the dielectric strength for c-C_4F_8 mixtures with CF_4, CO_2, N_2, O_2 and air by Boltzmann equation analysis," J. Phys. D: Appl. Phys. **47**(42), 425204 (2014).
[196] Y. Deng, B. Li, and D. Xiao, "Analysis of the insulation characteristics of C_3F_8 gas mixtures with N_2 and CO_2 using Boltzmann equation method," IEEE Trans. Dielectr. Electr. Insul. **22**(6), 3253–3259 (2015).
[197] Z. Xiaoling, J. Juntao, I. Bing, and X. Dengming, "The electronegativity analysis of c-C_4F_8 as a potential insulation substitute of SF_6," Plasma Sci. Technol. **18**(3), 292–298 (2016).
[198] M. Koch and C. M. Franck, "Partial discharges and breakdown in C_3F_8," J. Phys. D: Appl. Phys. **47**(40), 405203 (2014).
[199] M. Koch and C. M. Franck, "Prediction of partial discharge and breakdown voltages in CF_4 for arbitrary electrode geometries," J. Phys. D: Appl. Phys. **48**(5), 055207 (2015).
[200] X. Wang, L. Zhong, J. Yan, A. Yang, G. Han, G. Han, and M. Rong, "Investigation of dielectric properties of cold C_3F_8 mixtures and hot C_3F_8 gas as Substitutes for SF_6," Eur. Phys. J. D **69**(10), 240 (2015).
[201] Y. Wu, W. Wang, M. Rong, L. Zhong, J. Spencer, and J. Yan, "Prediction of critical dielectric strength of hot CF_4 gas in the temperature range of 300-3500 K," IEEE Trans. Dielectr. Electr. Insul. **21**(1), 129–137 (2014).
[202] V. A. Lisovskiy, V. A. Derevianko, and V. D. Yegorenkov, "DC breakdown in low-pressure CF_4," J. Phys. D: Appl. Phys. **48**(47), 475201 (2015).
[203] W. Wang, M. Rong, Y. Wu, J. W. Spencer, and J. D. Yan, "Transport coefficients of high temperature CF_4, C_2F_6, and C_3F_8 as candidate of SF_6," in *2011 1st International Conference on Electric Power Equipment-Switching Technology* (IEEE, 2011), pp. 621–625.
[204] W. Wang, Y. Wu, M. Rong, L. Éhn, and I. Černušák, "Theoretical computation of thermophysical properties of high-temperature F_2, CF_4, C_2F_2, C_2F_4, C_2F_6, C_3F_6 and C_3F_8 plasmas," J. Phys. D: Appl. Phys. **45**(28), 285201 (2012).
[205] L. Kang, N. Wenhao, L. Tao, Z. Guoqiang, and X. Haijiang, "Study of the decomposition of c-C_4F_8 and its mixture with N_2 under 50 Hz ac corona discharge," in *2013 Annual Report Conference on Electrical Insulation and Dielectric Phenomena* (IEEE, 2013), pp. 1229–1232.
[206] S. Solomon, J. B. Burkholder, A. R. Ravishankara, and R. R. Garcia, "Ozone depletion and global warming potentials of CF_3I," J. Geophys. Res.: Atmos. **99**(D10), 20929–20935, https://doi.org/10.1029/94jd01833 (1994).
[207] M. K. Donnelly, R. H. Harris, and J. C. Yang, *CF_3I Stability under Storage* (US Department of Commerce, Technical Administration, National Institute of Standards and Technology, 2004).
[208] S. Xiao, X. Zhang, Y. Han, and Q. Dai, "AC breakdown characteristics of CF_3I/N_2 in a non-uniform electric field," IEEE Trans. Dielectr. Electr. Insul. **23**(5), 2649–2656 (2016).
[209] X. Zhang, S. Xiao, Y. Han, and Q. Dai, "Analysis of the feasibility of CF_3I/CO_2 used in C-GIS by partial discharge inception voltages in positive half cycle and breakdown voltages," IEEE Trans. Dielectr. Electr. Insul. **22**(6), 3234–3243 (2015).
[210] H. Toyota, S. Matsuoka, and K. Hidaka, "Measurement of sparkover voltage and time lag characteristics in CF_3I-N_2 and CF_3I-air gas mixtures by using steep-front square voltage," IEEJ Trans. Fundam. Mater. **125**, 409–414 (2005).
[211] Z. Yuan, Y. Tu, C. Wang, S. Wang, Y. Cheng, and X. Dong, "Vapor-liquid equilibria of (CF_3I+ CO_2) at the temperature of 243.150 K," in *2015 IEEE 11th International Conference on the Properties and Applications of Dielectric Materials (ICPADM)* (IEEE, 2015), pp. 660–663.
[212] M. S. Kamarudin, L. Chen, P. Widger, K. H. Elnaddab, M. Albano, H. Griffiths, and A. Haddad, "CF_3I gas and its mixtures: Potential for electrical insulation," in *Proceedings of the CIGRE Session* (CIGRE, 2014), Vol. 45.
[213] T. Youping, L. Yan, W. Cong, L. Shan, and C. Yangchun, "Breakdown characteristics of CF_3I and CF_3I/N_2 gas mixtures in uniform field," in *2015 IEEE 11th International Conference on the Properties and Applications of Dielectric Materials (ICPADM)* (IEEE, 2015), pp. 520–523.
[214] P. Widger, A. Haddad, and H. Griffiths, "Breakdown performance of vacuum circuit breakers using alternative CF_3I-CO_2 insulation gas mixture," IEEE Trans. Dielectr. Electr. Insul. **23**(1), 14–21 (2016).
[215] L. Chen, P. Widger, M. S. Kamarudin, H. Griffiths, and A. Haddad, "Potential of CF_3I gas mixture as an insulation medium in gas-insulated equipment," in *2015 IEEE Conference on Electrical Insulation and Dielectric Phenomena (CEIDP)* (IEEE, 2015), pp. 868–871.
[216] L. Chen, P. Widger, M. S. Kamarudin, H. Griffiths, and A. Haddad, "CF_3I gas mixtures: Breakdown characteristics and potential for electrical insulation," IEEE Trans. Power Delivery **32**(2), 1089–1097 (2017).

[217] X. Zhang, S. Tian, S. Xiao, Y. Li, Z. Deng, and J. Tang, "Experimental studies on the power–frequency breakdown voltage of $CF_3I/N_2/CO_2$ gas mixture," J. Appl. Phys. **121**(10), 103303 (2017).

[218] J. de Urquijo, A. M. Juárez, E. Basurto, and J. L. Hernández-Ávila, "Electron impact ionization and attachment, drift velocities and longitudinal diffusion in CF_3I and CF_3I–N_2 mixtures," J. Phys. D: Appl. Phys. **40**(7), 2205 (2007).

[219] S. Kawaguchi, K. Satoh, and H. Itoh, "Electron transport in CF_3I and CF_3I/N_2 mixtures," Eur. Phys. J. D **68**(4), 100 (2014).

[220] M. Kimura and Y. Nakamura, "Electron swarm parameters in CF3I and a set of electron collision cross sections for the CF_3I molecule," J. Phys. D: Appl. Phys. **43**(14), 145202 (2010).

[221] X. Li, H. Zhao, J. Wu, and S. Jia, "Analysis of the insulation characteristics of CF_3I mixtures with CF_4, CO_2, N_2, O_2 and air," J. Phys. D: Appl. Phys. **46**(34), 345203 (2013).

[222] D. Yun-Kun and X. Deng-Ming, "The effective ionization coefficients and electron drift velocities in gas mixtures of CF_3I with N_2 and CO_2 obtained from Boltzmann equation analysis," Chin. Phys. B **22**(3), 035101 (2013).

[223] Y. Deng and D. Xiao, "Analysis of the insulation characteristics of CF_3I gas mixtures with Ar, Xe, He, N_2, and CO_2 using Boltzmann equation method," Jpn. J. Appl. Phys., Part 1 **53**(9), 096201 (2014).

[224] X. Li, "Numerical study of point-to-plane streamer discharge in CF_3I," J. Phys.: Conf. Ser. **418**(1), 012012 (2013).

[225] M. Taki, D. Maekawa, H. Odaka, H. Mizoguchi, and S. Yanabu, "Interruption capability of CF_3I Gas as a substitution candidate for SF_6 gas," IEEE Trans. Dielectr. Electr. Insul. **14**(2), 341–346 (2007).

[226] H. Katagiri, H. Kasuya, H. Mizoguchi, and S. Yanabu, "BTF interruption capability of CF_3I-CO_2 mixture," in *2008 17th International Conference on Gas Discharges and Their Applications* (IEEE, 2008), pp. 105–108.

[227] H. Katagiri, H. Kasuya, H. Mizoguchi, and S. Yanabu, "Investigation of the performance of CF_3I gas as a possible substitute for SF_6," IEEE Trans. Dielectr. Electr. Insul. **15**(5), 1424–1429 (2008).

[228] Y. Yokomizu, R. Ochiai, and T. Matsumura, "Electrical and thermal conductivities of high-temperature CO_2-CF_3I mixture and transient conductance of residual arc during its extinction process," J. Phys. D: Appl. Phys. **42**(21), 215204 (2009).

[229] Y. Cressault, V. Connord, H. Hingana, P. Teulet, and A. Gleizes, "Transport properties of CF_3I thermal plasmas mixed with CO_2, air or N_2 as an alternative to SF_6 plasmas in high-voltage circuit breakers," J. Phys. D: Appl. Phys. **44**(49), 495202 (2011).

[230] M. N. Ngoc, A. Denat, N. Bonifaci, O. Lesaint, W. Daoud, and M. Hassanzadeh, "Electrical breakdown of CF_3I and CF_3I-N_2 gas mixtures," in *2009 IEEE Conference on Electrical Insulation and Dielectric Phenomena* (IEEE, 2009), pp. 557–560.

[231] H. Kasuya, Y. Kawamura, H. Mizoguchi, Y. Nakamura, S. Yanabu, and N. Nagasaki, "Interruption capability and decomposed gas density of CF_3I as a substitute for SF_6 gas," IEEE Trans. Dielectr. Electr. Insul. **17**(4), 1196–1203 (2010).

[232] H. Kasuya, H. Katagiri, Y. Kawamura, D. Saruhashi, Y. Nakamura, H. Mizoguchi, and S. Yanabu, "Measurement of decomposed gas density of CF_3I-CO_2 mixture," in *Proceedings of the 16th International Symposium on High Voltage Engineering (ISH)* (SAIEE, Innes House, Johannesburg, 2009), pp. 744–747.

[233] T. Takeda, S. Matsuoka, A. Kumada, and K. Hidaka, "Insulation performance of CF_3I and its by-products by sparkover discharge," in *The International Conference on Electrical Engineering* (ICEE, 2008), pp. 1–6.

[234] M. S. Kamarudin, A. Haddad, B. C. Kok, and N. A. M. Jamail, "Pressurized CF_3I-CO_2 gas mixture under lightning impulse and its solid by-products," Int. J. Electr. Comput. Eng. **7**(6), 3088 (2017).

[235] P. Widger and A. Haddad, "Solid by-products of a CF_3I-CO_2 insulating gas mixtures on electrodes after lightning impulse breakdown," J. Phys. Commun. **1**(2), 025010 (2017).

[236] M. S. Kamarudin, M. Albano, P. Coventry, N. Harid, and A. Haddad, "A survey on the potential of CF_3I gas as an alternative for SF_6 in high voltage applications," in *45th International Universities Power Engineering Conference, UPEC2010* (IEEE, 2010), pp. 1–5.

[237] M. K. M. Jamil, S. Ohtsuka, M. Hikita, H. Saitoh, and M. Sakaki, "Gas by-products of CF_3I under AC partial discharge," J. Electrostat. **69**(6), 611–617 (2011).

[238] X. Zhang, S. Xiao, J. Zhang, C. Li, Q. Dai, and Y. Han, "Influence of humidity on the decomposition products and insulating characteristics of CF_3I," IEEE Trans. Dielectr. Electr. Insul. **23**(2), 819–828 (2016).

[239] S. Xiao, Y. Li, X. Zhang, J. Tang, S. Tian, and Z. Deng, "Formation mechanism of CF_3I discharge components and effect of oxygen on decomposition," J. Phys. D: Appl. Phys. **50**(15), 155601 (2017).

[240] H. E. Nechmi, A. Beroual, A. Girodet, and P. Vinson, "Fluoronitriles/CO_2 gas mixture as promising substitute to SF_6 for insulation in high voltage applications," IEEE Trans. Dielectr. Electr. Insul. **23**(5), 2587–2593 (2016).

[241] J. G. Owens, "Greenhouse gas emission reductions through use of a sustainable alternative to SF_6," in *2016 IEEE Electrical Insulation Conference (EIC)* (IEEE, 2016), pp. 535–538.

[242] C. Preve, R. Maladen, and D. Piccoz, "Method for validation of new eco-friendly insulating gases for medium voltage equipment," in *2016 IEEE International Conference on Dielectrics (ICD)* (IEEE, 2016), Vol. 1, pp. 235–240.

[243] Y. Kieffel, T. Irwin, P. Ponchon, and J. Owens, "Green gas to replace SF_6 in electrical grids," IEEE Power Energy Mag. **14**(2), 32–39 (2016).

[244] Y. Li, X. Zhang, J. Zhang, C. Xie, X. Shao, Z. Wang, D. Chen, and S. Xiao, "Study on the thermal decomposition characteristics of C_4F_7N-CO_2 mixture as eco-friendly gas insulating medium," High Voltage **5**(1), 46–52 (2020).

[245] Y. Li, X. Zhang, Q. Chen, J. Zhang, Y. Li, S. Xiao, and J. Tang, "Influence of oxygen on dielectric and decomposition properties of C_4F_7N-N_2-O_2 mixture," IEEE Trans. Dielectr. Electr. Insul. **26**(4), 1279–1286 (2019).

[246] C. Preve, R. Maladen, and D. Picco, "Alternative gases to SF_6 as breaking medium for switching performance: Measurement of the concentrations of by-products and assessment of the acute toxicity," in 21st International Symposium on High Voltage Engineering, Budapest, Hungary, August 2019.

[247] M. P. Sulbaek Andersen, M. Kyte, S. T. Andersen, C. J. Nielsen, and O. J. Nielsen, "Atmospheric chemistry of $(CF_3)_2CFCN$: A replacement compound for the most potent industrial greenhouse gas, SF_6," Environ. Sci. Technol. **51**(3), 1321–1329 (2017).

[248] S. Blázquez, M. Antiñolo, O. J. Nielsen, J. Albaladejo, and E. Jiménez, "Reaction kinetics of $(CF_3)_2CFCN$ with OH radicals as a function of temperature (278–358 K): A good replacement for greenhouse SF_6," Chem. Phys. Lett. **687**, 297–302 (2017).

[249] X. Zhang, Y. Li, D. Chen, S. Xiao, S. Tian, J. Tang, and R. Zhuo, "Reactive molecular dynamics study of the decomposition mechanism of the environmentally friendly insulating medium C_3F_7CN," RSC Adv. **7**(80), 50663–50671 (2017).

[250] Y. Li, X. Zhang, S. Xiao, Q. Chen, J. Tang, D. Chen, and D. Wang, "Decomposition properties of C_4F_7N/N_2 gas mixture: An environmentally friendly gas to replace SF_6," Ind. Eng. Chem. Res. **57**(14), 5173–5182 (2018).

[251] Y. Li, X. Zhang, J. Zhang, S. Xiao, B. Xie, D. Chen, Y. Gao, and J. Tang, "Assessment on the toxicity and application risk of C_4F_7N: A new SF_6 alternative gas," J. Hazard. Mater. **368**, 653–660 (2019).

[252] X. Zhang, Y. Li, S. Xiao, S. Tian, Z. Deng, and J. Tang, "Theoretical study of the decomposition mechanism of environmentally friendly insulating medium C_3F_7CN in the presence of H_2O in a discharge," J. Phys. D: Appl. Phys. **50**(32), 325201 (2017).

[253] X. Zhang, Y. Li, D. Chen, S. Xiao, S. Tian, J. Tang, and D. Wang, "Dissociative adsorption of environment-friendly insulating medium C_3F_7CN on Cu (111) and Al (111) surface: A theoretical evaluation," Appl. Surf. Sci. **434**, 549–560 (2018).

[254] Y. Li, X. Zhang, Q. Chen, J. Zhang, D. Chen, Z. Cui, S. Xiao, and J. Tang, "Study on the thermal interaction mechanism between C_4F_7N-N_2 and copper, aluminum," Corros. Sci. **153**, 32–46 (2019).

[255] J. D. Mantilla, N. Gariboldi, S. Grob, and M. Claessens, "Investigation of the insulation performance of a new gas mixture with extremely low GWP," in *2014 IEEE Electrical Insulation Conference (EIC)* (IEEE, 2014), pp. 469–473.

[256] P. Simka and N. Ranjan, "Dielectric strength of C_5 perfluoroketone," in *Proceedings of the 19th International Symposium on High Voltage Engineering* (Pilsen, Czech Republic, 2015), pp. 23–28.
[257] M. Saxegaard, M. Kristoffersen, P. Stoller, M. Seeger, M. Hyrenbach, and H. Landsverk, Dielectric Properties of Gases Suitable for Secondary Medium Voltage Switchgear, CIRED Paper No. 926, 2015.
[258] M. Hyrenbach and S. Zache, "Alternative insulation gas for medium-voltage switchgear," in *2016 Petroleum and Chemical Industry Conference Europe (PCIC Europe)* (IEEE, 2016), pp. 1–9.
[259] Y. Wu, C. Wang, H. Sun, M. Rong, A. B. Murphy, T. Li, J. Zhong, Z. Chen, F. Yang, and C. Niu, "Evaluation of SF_6-alternative gas C5-PFK based on arc extinguishing performance and electric strength," J. Phys. D: Appl. Phys. **50**(38), 385202 (2017).
[260] L. Zhong, M. Rong, X. Wang, J. Wu, G. Han, G. Han, Y. Lu, A. Yang, and Y. Wu, "Compositions, thermodynamic properties, and transport coefficients of high-temperature $C_5F_{10}O$ mixed with CO_2 and O_2 as substitutes for SF_6 to reduce global warming potential," AIP Adv. **7**(7), 075003 (2017).
[261] A. V. Tatarinov, I. V. Bilera, S. V. Avtaeva, V. A. Shakhatov, P. V. Solomakhin, R. Maladen, C. Prévé, and D. Piccoz, "Dielectric barrier discharge processing of trans-CF_3CH=CHF and $CF_3C(O)CF(CF_3)_2$, their mixtures with air, N_2, CO_2 and analysis of their decomposition products," Plasma Chem. Plasma Process. **35**(5), 845–862 (2015).
[262] X. Zhang, Y. Li, S. Xiao, J. Tang, S. Tian, and Z. Deng, "Decomposition mechanism of $C_5F_{10}O$: An environmentally friendly insulation medium," Environ. Sci. Technol. **51**(17), 10127–10136 (2017).
[263] X. Zhang, Y. Li, S. Tian, S. Xiao, D. Chen, J. Tang, and R. Zhuo, "Decomposition mechanism of the C5-PFK/CO_2 gas mixture as an alternative gas for SF_6," Chem. Eng. J. **336**, 38–46 (2018).
[264] S. Xiao, Y. Li, X. Zhang, S. Tian, Z. Deng, and J. Tang, "Effects of micro-water on decomposition of the environment-friendly insulating medium $C_5F_{10}O$," AIP Adv. **7**(6), 065017 (2017).
[265] M. Hyrenbach, T. A. Paul, and J. Owens, "Environmental and safety aspects of airplus insulated GIS," CIRED-Open Access Proc. J. **2017**(1), 132–135.
[266] S. Tian, X. Zhang, Y. Wang, X. Rao, F. Ye, Y. Li, and S. Xiao, "Partial discharge characteristics of $C_6F_{12}O/CO_2$ mixed gas at power frequency AC voltage," AIP Adv. **9**(9), 095057 (2019).
[267] S. Tian, X. Zhang, S. Xiao, J. Zhang, Q. Chen, and Y. Li, "Application of $C_6F_{12}O/CO_2$ mixture in 10 kV medium-voltage switchgear," IET Sci., Meas. Technol. **13**(9), 1225–1230 (2019).
[268] L. Cheng, X. Yu, K. Zhao, H. Hou, and B. Wang, "Electronic structures and OH-induced atmospheric degradation of CF_3NSF_2: A potential green dielectric replacement for SF6," J. Phys. Chem. A **121**(13), 2610–2619 (2017).
[269] A. Chachereau, M. Rabie, and C. M. Franck, "Electron swarm parameters of the hydrofluoroolefine HFO1234ze," Plasma Sources Sci. Technol. **25**(4), 045005 (2016).
[270] A. Chachereau and C. M. Franck, "Characterization of HFO1234ze mixtures with N_2 and CO_2 for use as gaseous electrical insulation media," in *Proceedings of the 20th International Symposium on High Voltage Engineering (ISH 2017)* (Cigré, 2017).
[271] C. Preve, D. Piccoz, and R. Maladen, "Application of HFO1234zeE in MV switchgear AS SF_6 alternative gas," CIRED-Open Access Proc. J. **2017**(1), 42–45.
[272] Z. Chen, H. Zhang, Y. Shang, Q. Chen, B. Han, and Z. Li, "Theoretical study of OCCHCN as a potential alternative insulation gas for SF_6," AIP Adv. **7**(1), 015111 (2017).